

Applications

- Conventional electronics - CMOS
- Opto-electronics
 - Photonic crystals – bandgaps in artificially created regular crystal arrays
 - Lasers – multiple quantum well (MQW) lasers
- High power/temp. Electronics
 - GaN, SiC devices
- Microwave Electronics
 - InP, GaAs-based devices – high electron mobility transistors (HEMTs)

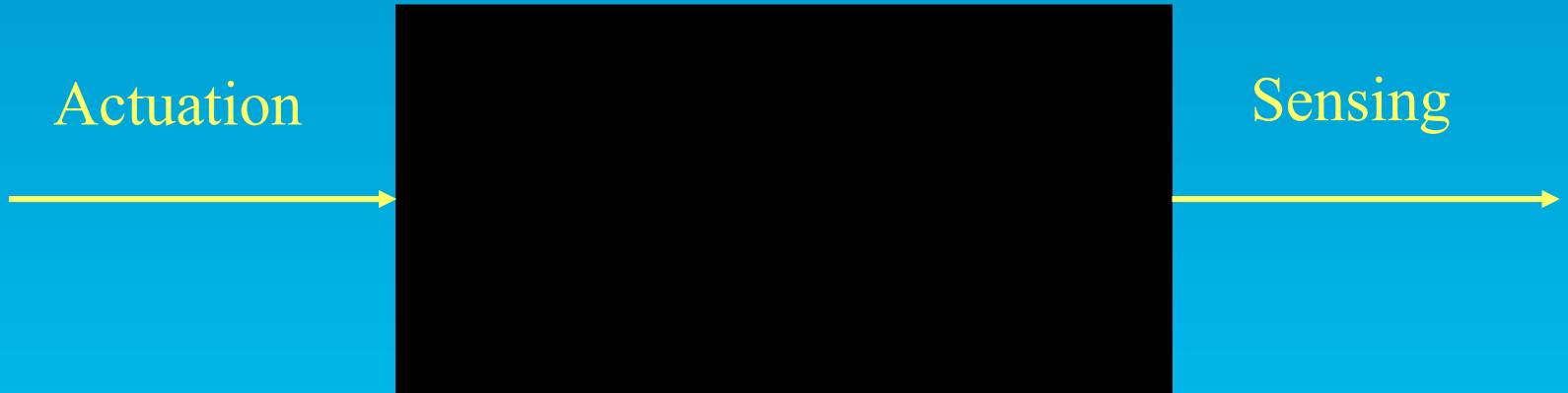
Applications

- Bio-electronics
 - neurons on silicon
- Quantum-effect devices
 - resonant tunneling, diffusive and ballistic transport devices, quantum information processing
- Molecular or single electronics
 - carbon nanotube transistors
- Micro-electro-mechanical systems
 - sensors, actuators, micro-pumps

MEMS

- Microelectromechanical systems
- Actuator
- Sensor

MEMS

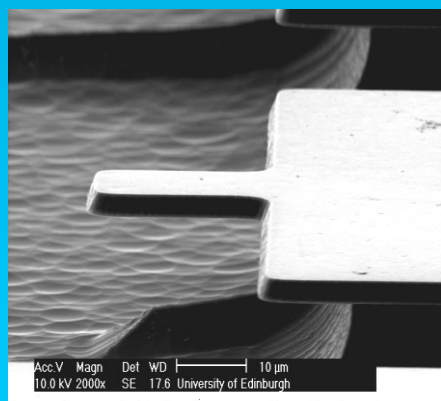
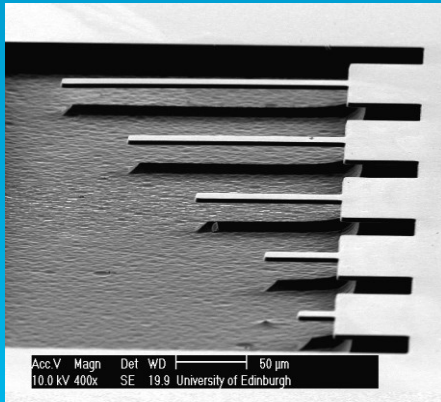


- Mechanisms
 - Electrostatic
 - Electrothermal
 - Piezoelectric
- Mechanisms
 - Capacitive
 - Piezoresistive
 - Piezoelectric

Devices and Systems

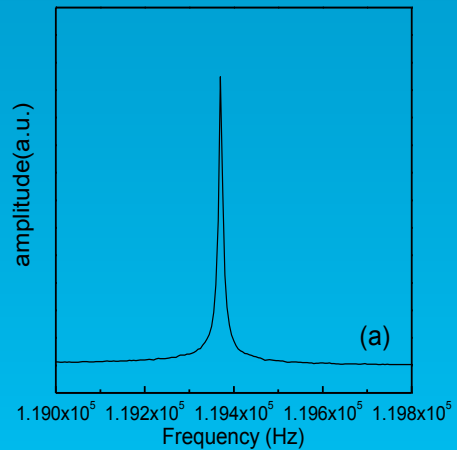
- For example
 - Resonators
 - Pressure sensors

Silicon carbide resonators



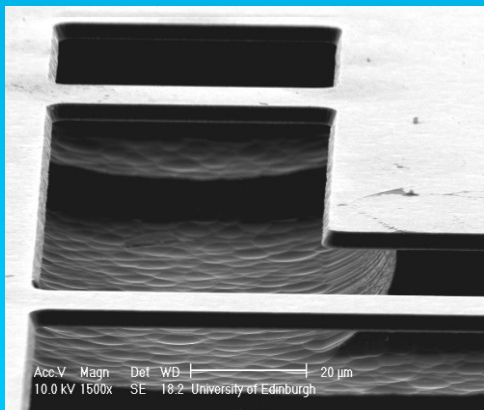
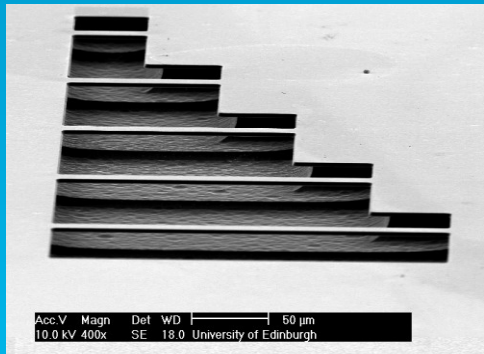
SEM image of a group of free standing cantilever beams with lengths of 25, 50, 100, 150, 200 μm and close-up image of cantilever of 25 μm long. All the beams are 15 μm wide and nominally 2 μm thick 3C-SiC on Si

*J. Vac. Sci. and
Technol., B21, 2998 -
3002, (2003)*

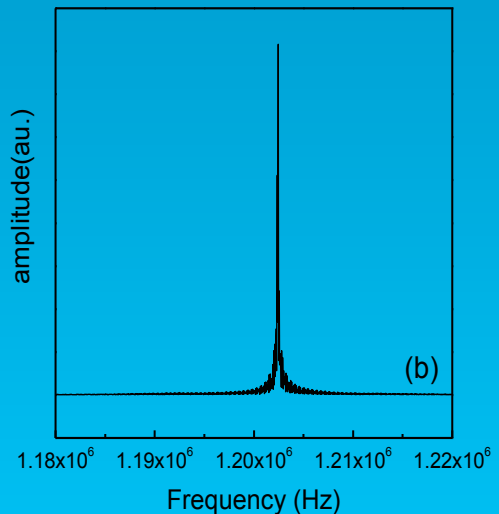


Measured fundamental resonance peak at 119.4kHz for 200 μm long cantilever

Silicon carbide bridge resonators



SEM image of bridges with lengths of 50, 100, 150, 200, 250 μm and close-up image of 50 μm and 100 μm long bridges. All the beams are 15 μm wide and nominally 2 μm thick 3C-SiC on Si
J. Vac. Sci. and Technol., B21, 2998 - 3002, (2003)



Measured fundamental resonance peak at 1.2MHz for 200 μm long bridge

Resonant frequency of beams

- General formula for the resonant frequencies of beams (vertical direction)

$$f_n = \frac{\lambda_n^2}{2\pi} \sqrt{\frac{E \cdot I}{\rho \cdot A \cdot L^4}} \quad (1)$$

n = mode number (0 = fundamental mode)

- cantilever: $\lambda_0 = 1.88$
- bridge: $\lambda_0 = 4.73$
- beam dimensions and parameters:
- w = width
- t = thickness
- L = length
- ρ = mass density
- E = Young's modulus

- I = moment of inertia of beams

$$I = \frac{w \cdot t^3}{12}$$

- A = cross – sectional area

$$A = w \cdot t$$

- Substituting I and A in (1)

$$f_n = \frac{\lambda_n^2 \cdot t}{2\pi \cdot L^2} \sqrt{\frac{E}{12\rho}}$$

MEMS - Resonant freq calculation – cantilever versus bridge

- Fundamental mode of cantilevers, $n = 0$ and $\lambda_0 = 1.88$:

$$f_0 = 0.162 \left(\frac{t}{L^2} \right) \sqrt{\frac{E}{\rho}}$$

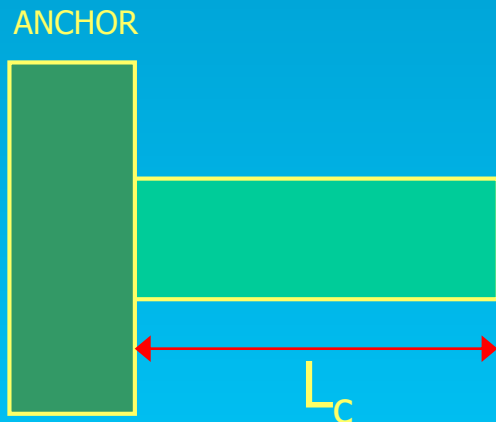
- Fundamental mode of bridges, $n = 0$ and $\lambda_0 = 4.73$:

$$f_0 = 1.03 \left(\frac{t}{L^2} \right) \sqrt{\frac{E}{\rho}}$$

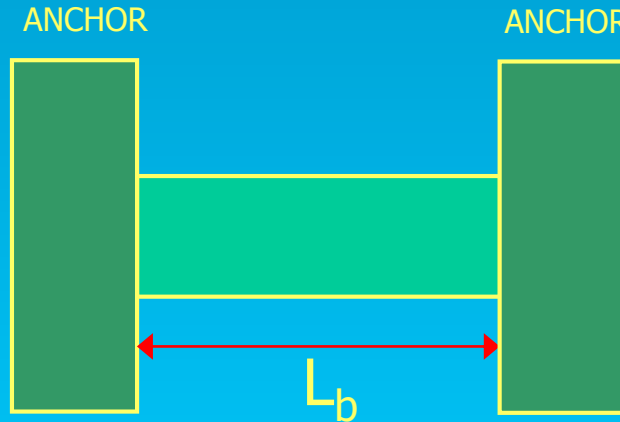
Resonator structure design

Maximise resonant frequency

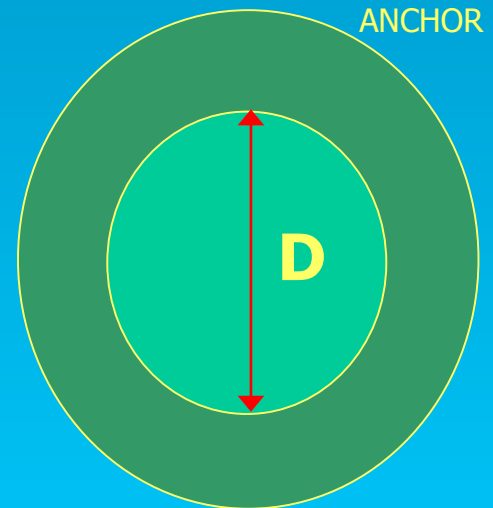
Cantilever



Bridge



Disk



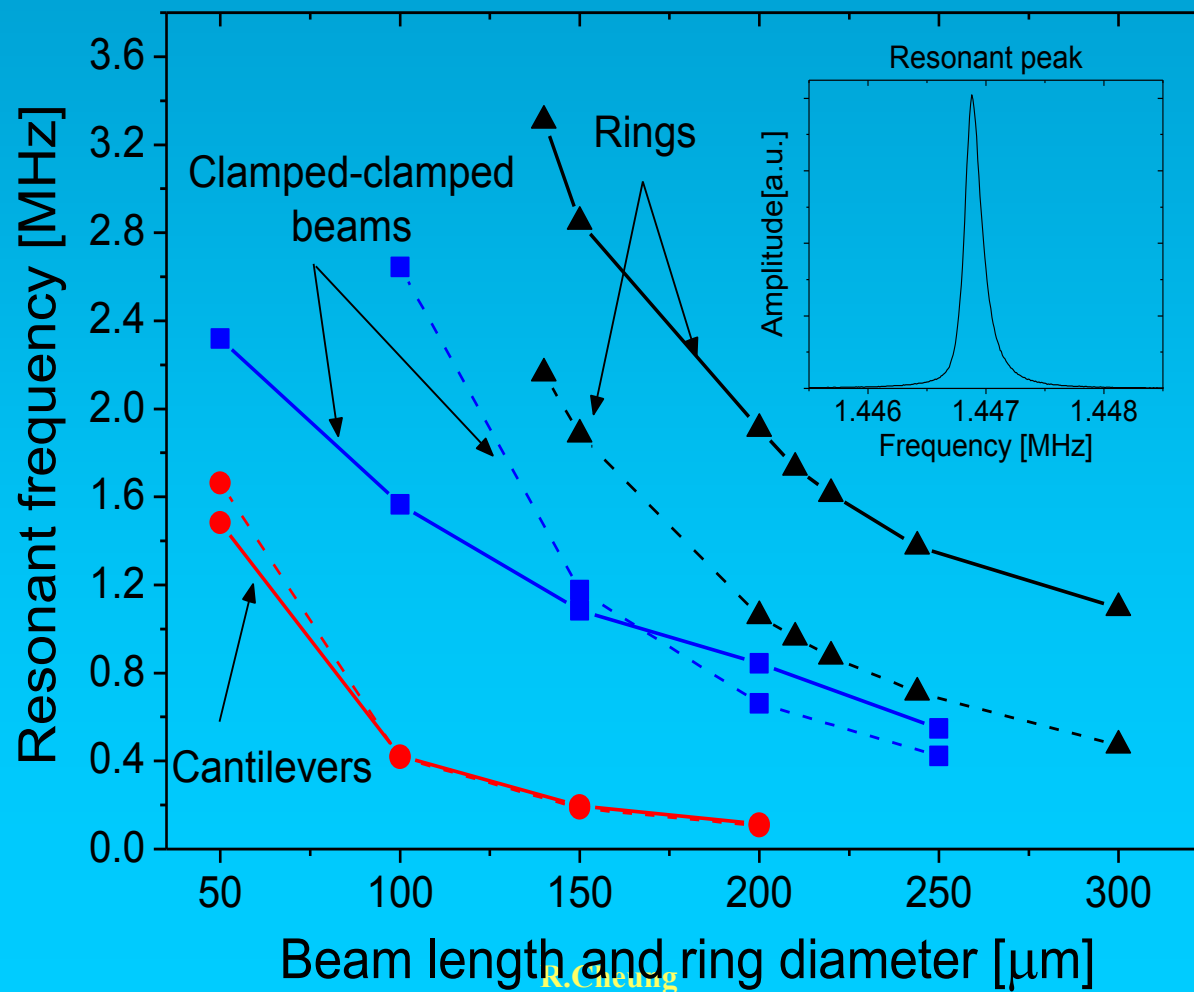
$$f_c = 0.162 \sqrt{\frac{E}{\rho}} \frac{t}{L_c^2}$$

$$f_b = 1.03 \sqrt{\frac{E}{\rho}} \frac{t}{L_b^2}$$

$$f_d = 1.65 \sqrt{\frac{E}{\rho}} \frac{t}{D^2}$$

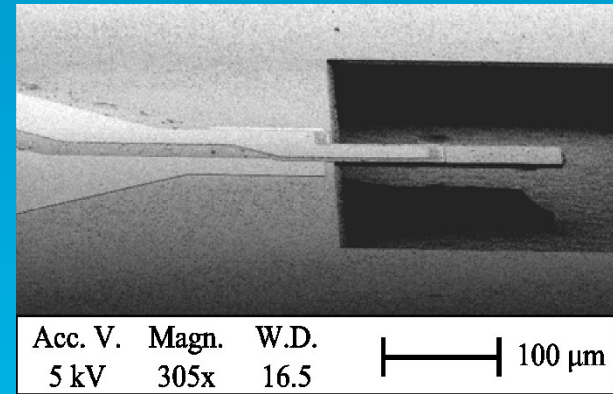
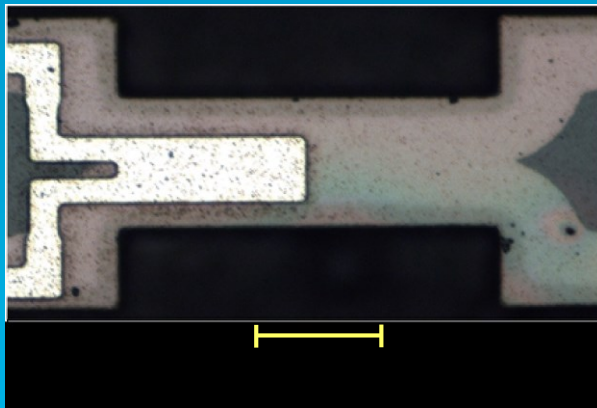
E = Young's Modulus; ρ = mass density

Mechanical actuation – Beam length L – ring diameter D – theory (dashed line) measurement (solid line) (inset: resonant peak detected at ~ 1.45 MHz for a SiC ring with $D = 250 \mu\text{m}$)

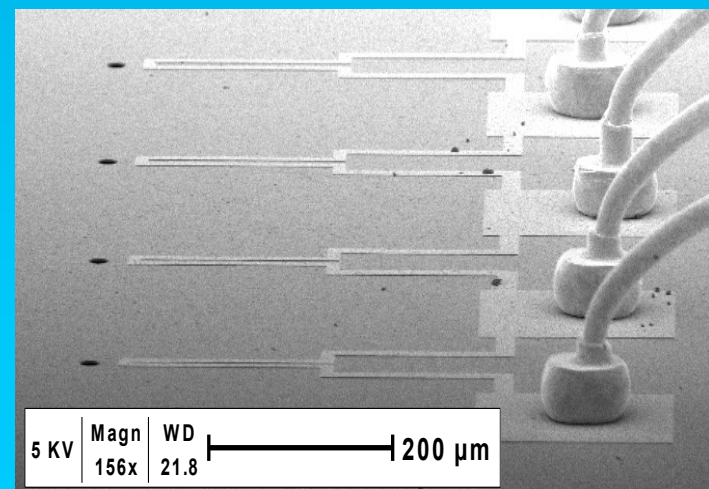
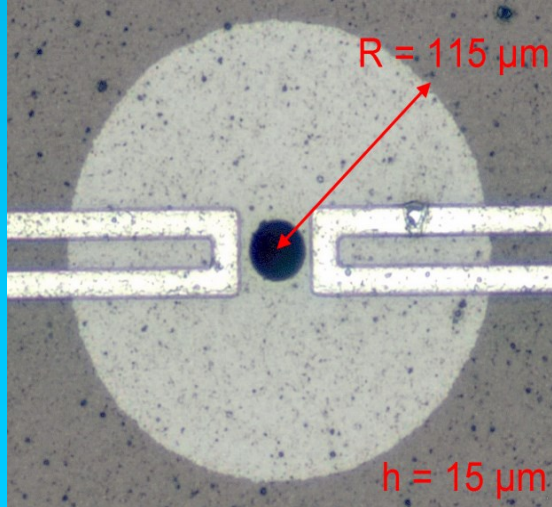
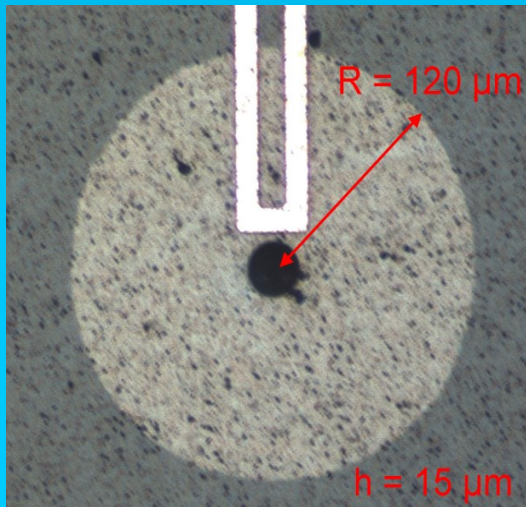


Examples of fabricated SiC devices

Beams



Rings



Devices with metal electrodes

Actuation methods

- Electrostatic
- Electro-thermal
- Piezo-electric

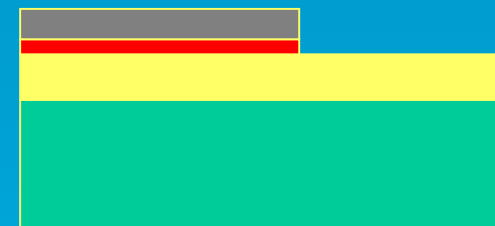
SiC MEMS fabrication process



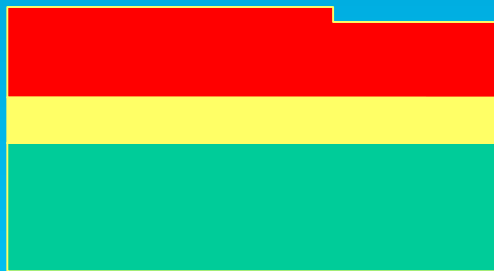
1) SiC growth on substrate



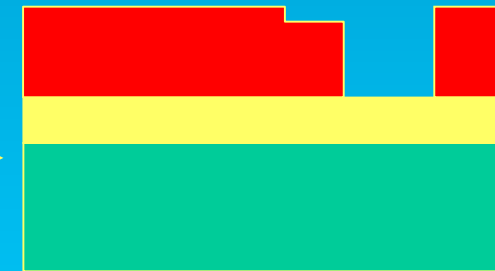
2) Thin oxide growth + metal sputtering



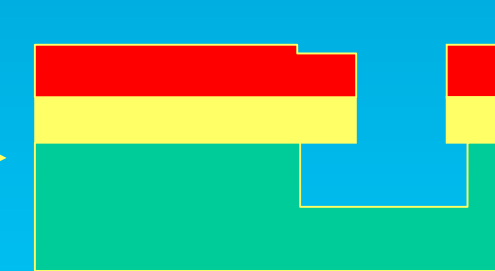
3) Metal etching (RIE): electrode patterning



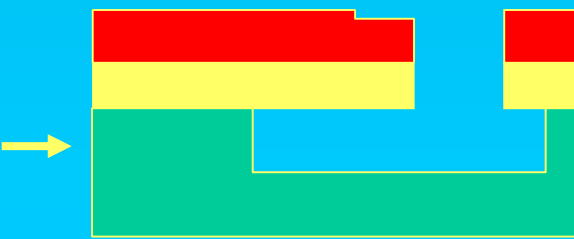
4) Oxide deposition (PECVD): mask



5) Oxide etching (RIE): structure shape



6) SiC etching and release (ICP-RIE)

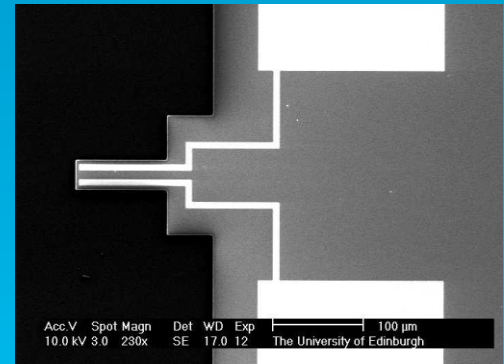
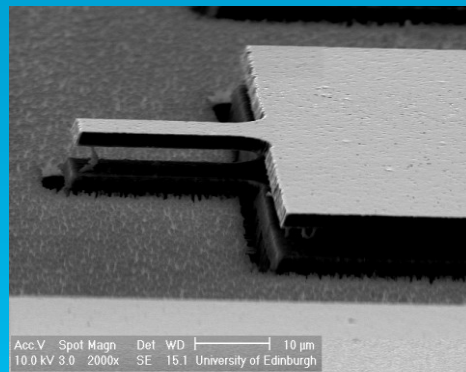
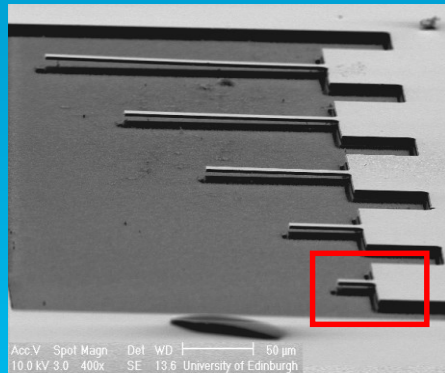


7) Final release (XeF_2
MDP⁴
vanolur)



8) Residual oxide removal
R.Cheung

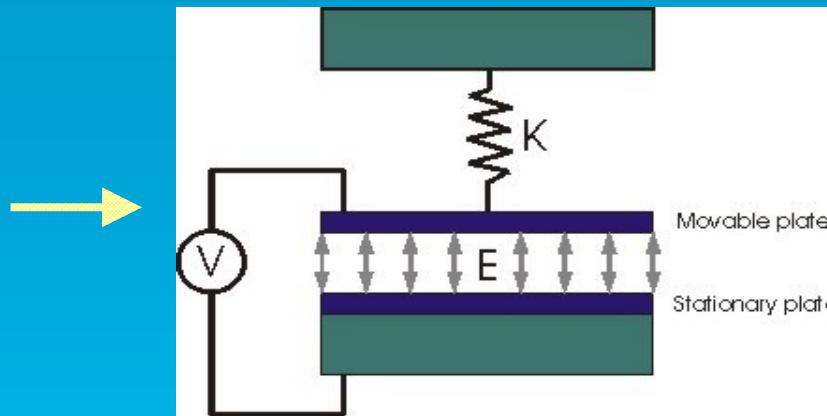
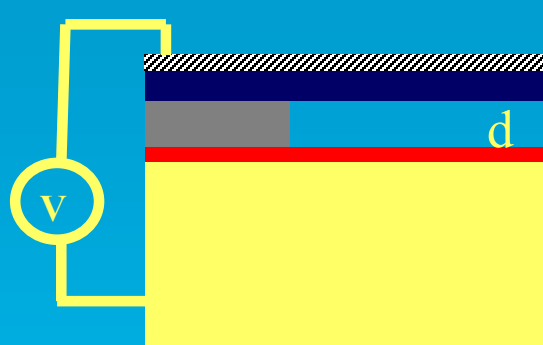
SiC electrostatic actuators



SEM images of a group of cantilevers with different length of 25, 50, 100, 150, 200 microns. All cantilevers are nominally 2 microns thick and 15 microns wide. NiCr on top of the actuators.

Microelectronic Engineering, 78-79, pp 106-111, (2005)

Electrostatic actuation



Electrostatic
actuation with
voltage control

$$F_{electrostatic} = \frac{V^2 \epsilon A}{2d^2} = kz$$

When applying an a.c. voltage with a d.c. component, the square of the voltage:

$$V^2 = (V_{ac} \sin \omega t + V_{dc})^2$$

$$= 2V_{ac}V_{dc} \sin \omega t + 0.5V_{ac}^2(1 - \cos 2\omega t) + V_{dc}^2$$

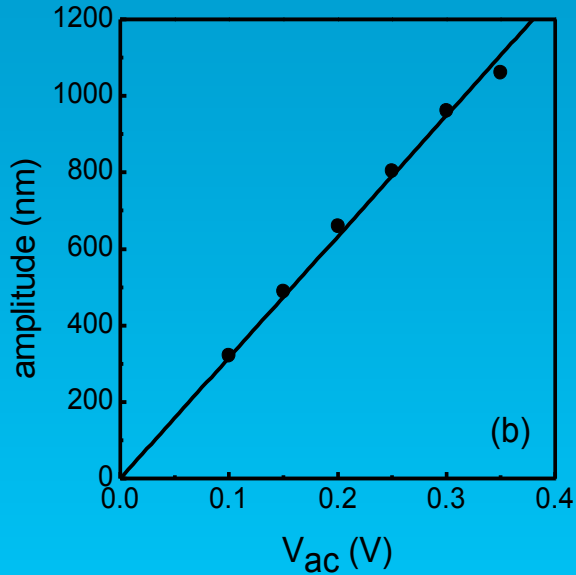
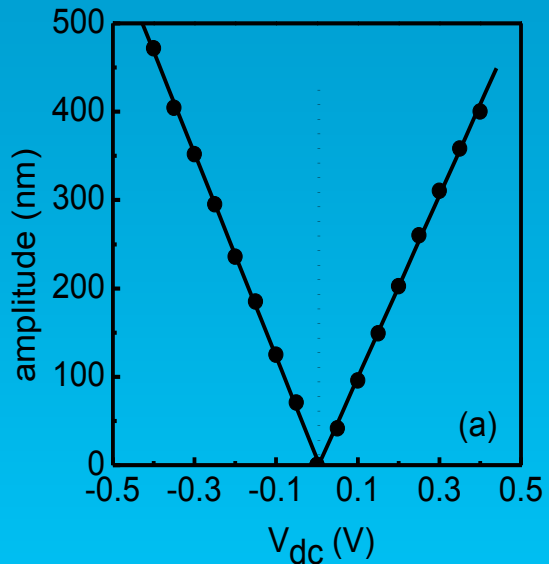
Contribute to the resonance

$$Z \propto V^2$$

$$Z \propto 2V_{ac}V_{dc} \text{ when } \omega = 2\pi f_0$$

$$V^2 \propto 2V_{ac}V_{dc} \text{ when } \omega = 2\pi f_0$$

Amplitude dependence on V_{dc} and V_{ac}



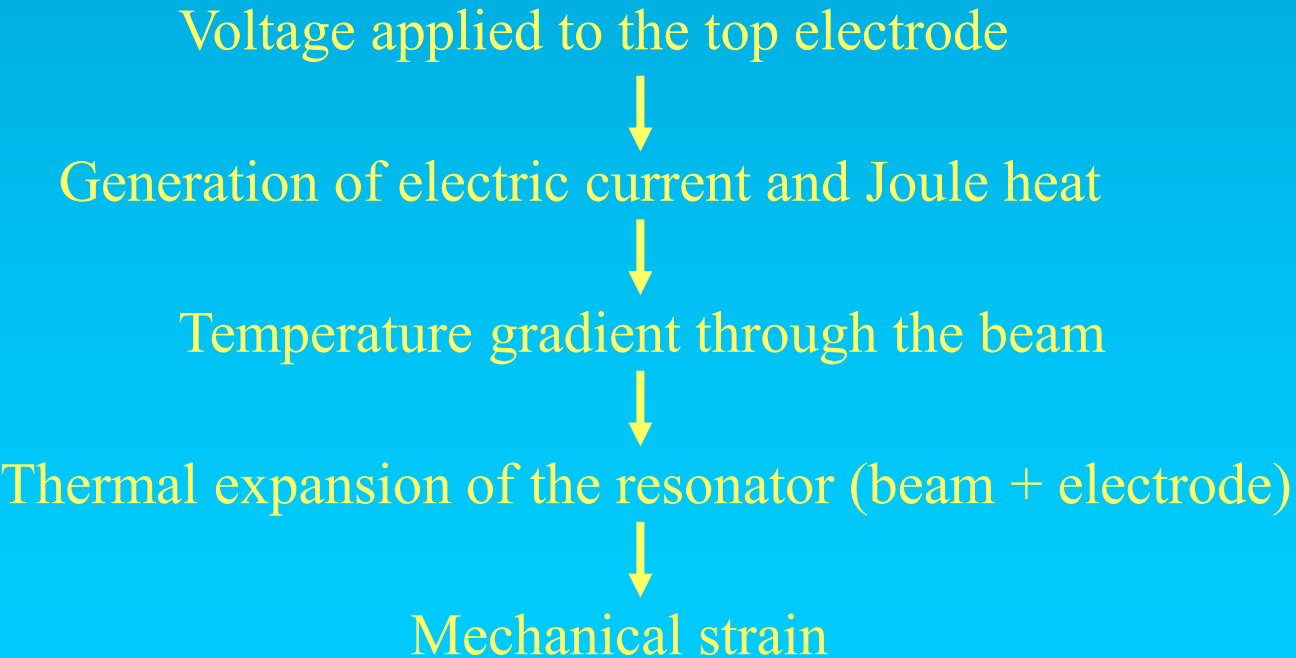
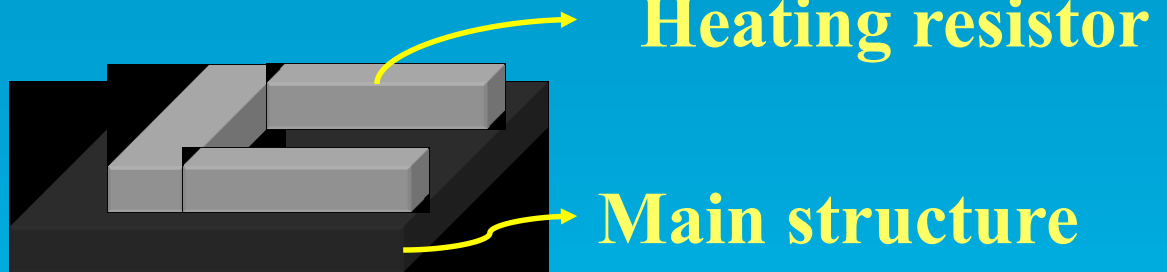
- Amplitude linearly depends on V_{dc} and V_{ac}
- Linearly fitted lines intersect the origin

Amplitude Z of a 200 microns long cantilever as a function of (a) V_{dc} ($V_{ac}=0.3\text{V}$) (b) V_{ac} ($V_{dc}=0.2\text{V}$). The frequency of the applied a.c. signal is 66.65KHz

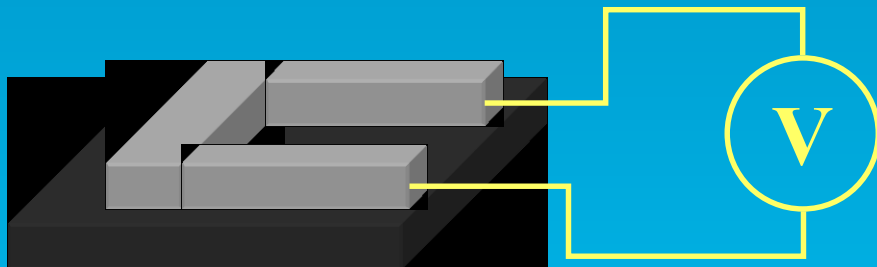
Microelectronic Engineering, 78-79, pp 106-111, (2005)

Electro-thermal actuation

Bimorph resonators:



Electro-thermal actuation



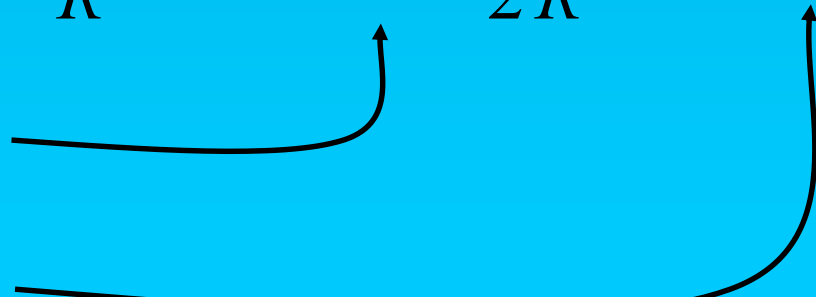
$$V = V_{dc} + V_{ac} \sin \omega t$$

DC: steady displacement
AC: vibration

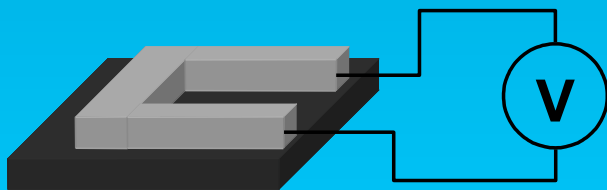
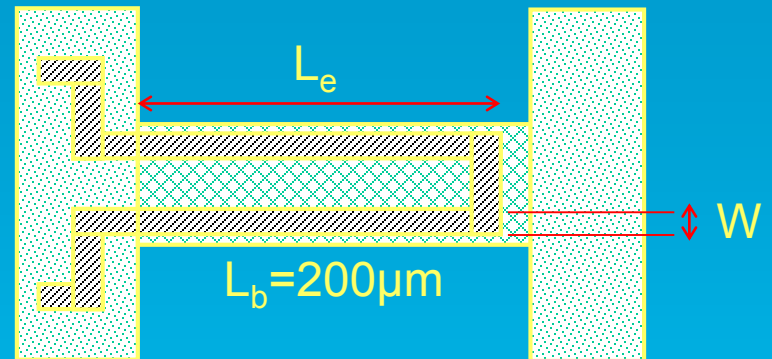
Force \propto Electric power dissipated in resistor

$$P = \frac{V^2}{R} - P_{ac} = \frac{2V_{dc}V_{ac}}{R} \sin \omega t - \frac{V_{ac}^2}{2R} \cos 2\omega t$$

Resonance: $f = \frac{\omega}{2\pi} = \begin{cases} f_0 \\ \frac{f_0}{2} \end{cases}$



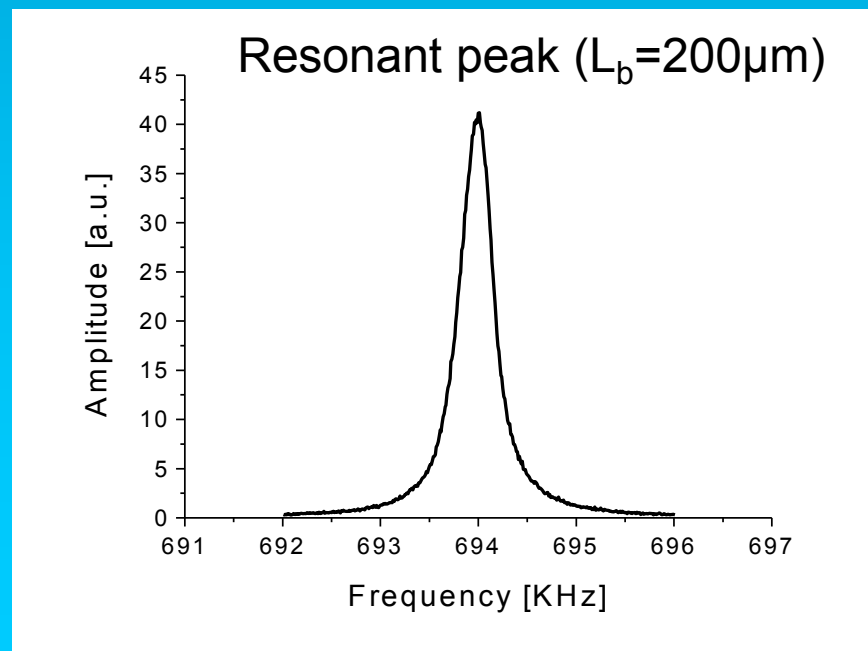
Electro-thermal actuation



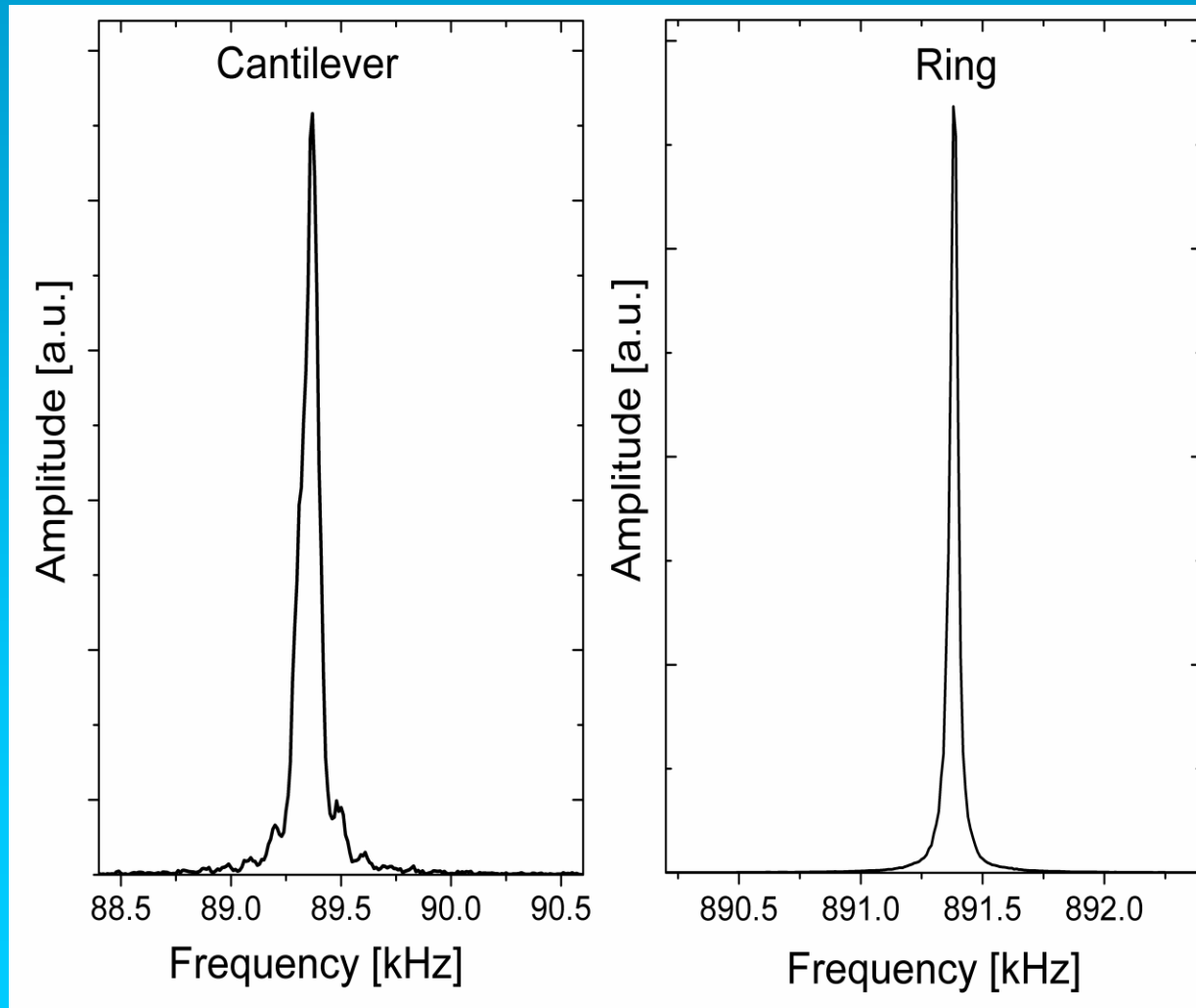
$$V = V_{dc} + V_{ac} \sin \omega t$$

$$V_{dc} = 1 \text{ V}$$

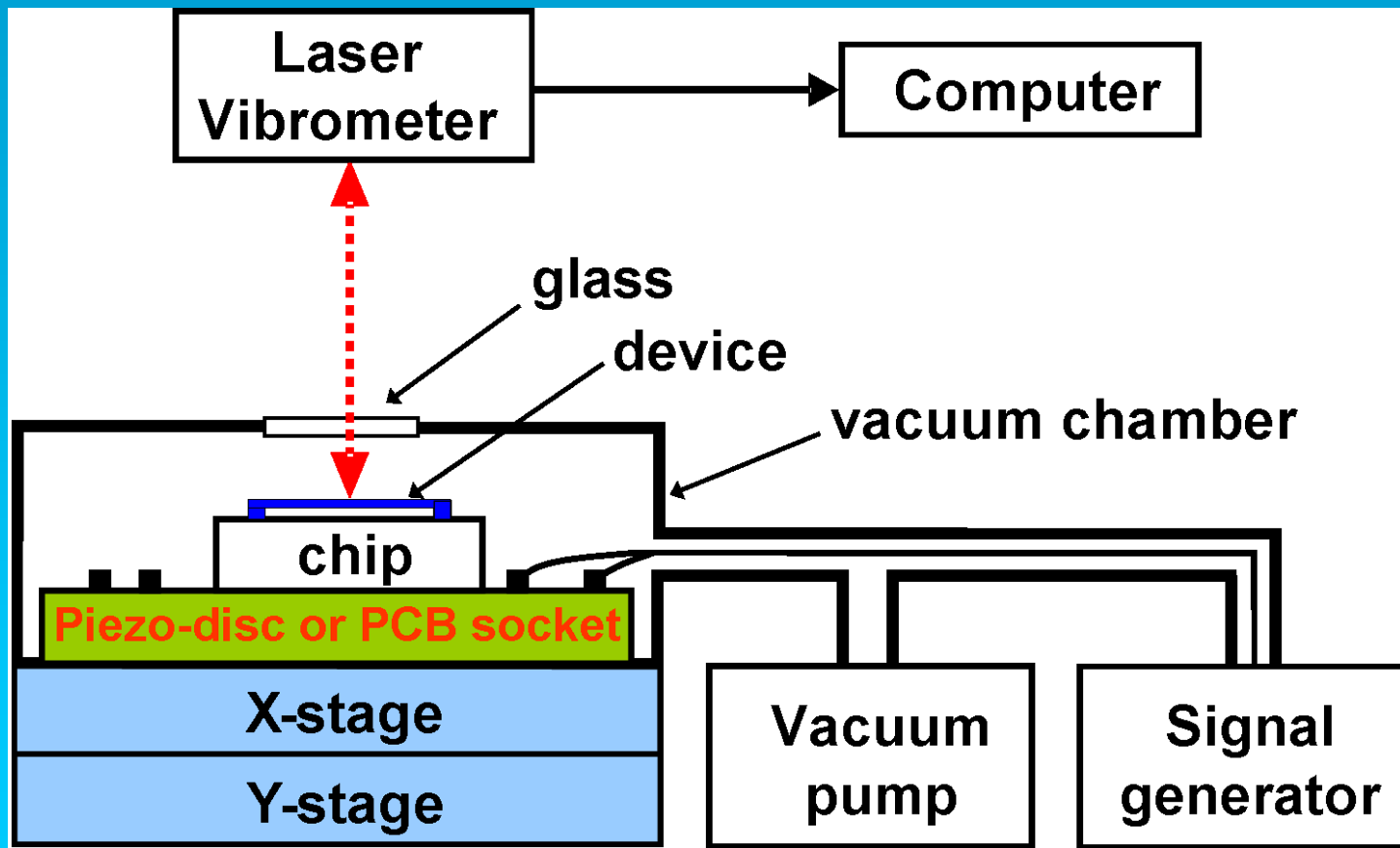
$$V_{ac} = 4 \text{ V}$$



Electro-thermal actuation measurements on Al/SiC structures: actuation resonant peaks for a cantilever ($L = 200 \mu\text{m}$) and a ring ($D = 190 \mu\text{m}$).

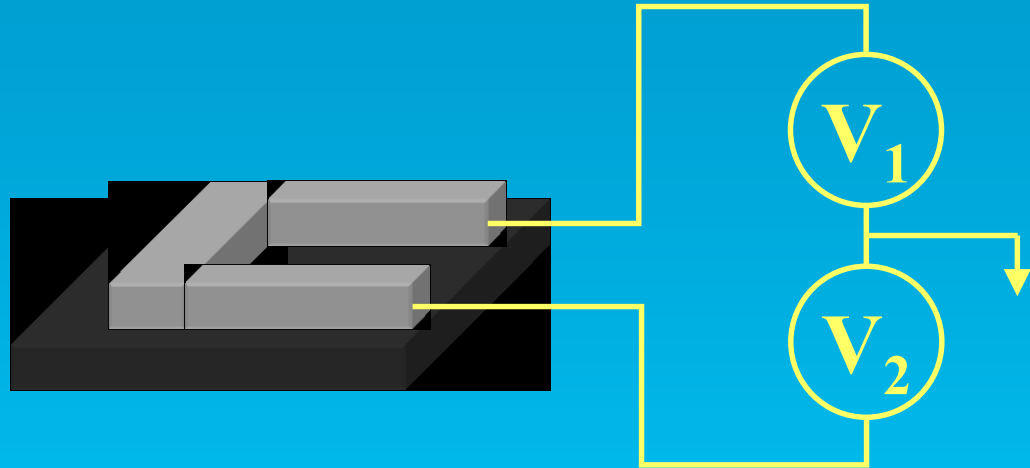


Measurement set-up - optical



Mechanical mixing

Mixing on MEMS



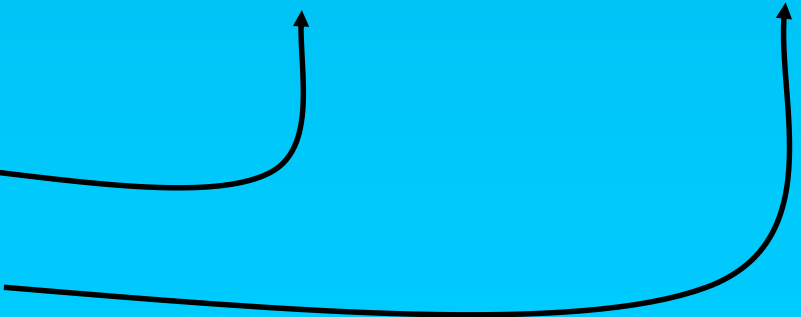
Two AC signals applied

$$f_1 = \frac{\omega_1}{2\pi}, f_2 = \frac{\omega_2}{2\pi}$$

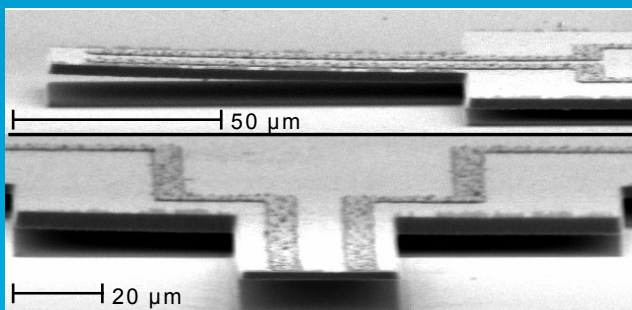
$$P = \frac{V^2}{R} - - > P_{ac} \alpha \frac{VV}{R} \left\{ \cos(\omega_1 - \omega_2)t - \cos(\omega_1 + \omega_2)t \right\}$$

Resonance:

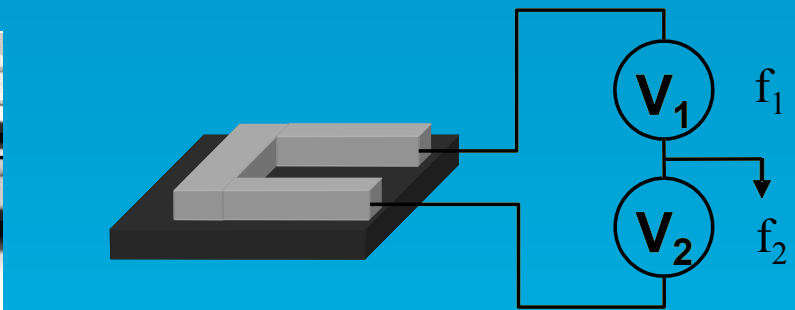
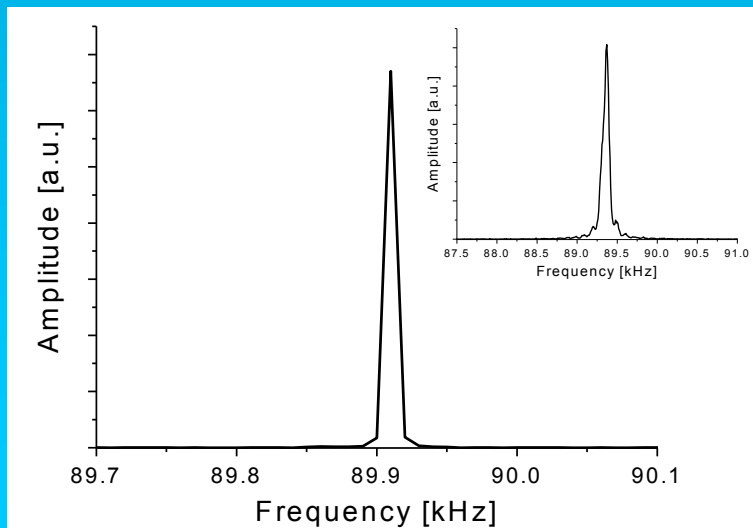
$$\begin{cases} f_1 - f_2 = f_0 \\ f_1 + f_2 = f_0 \end{cases}$$



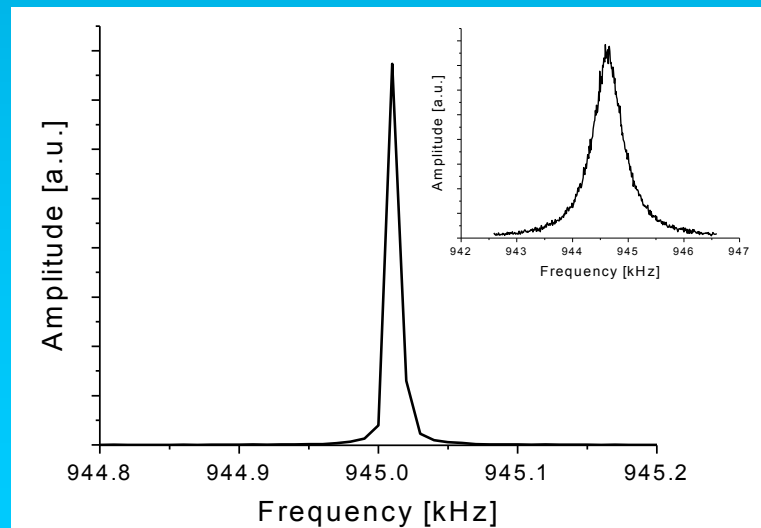
Electro-thermal mixing



SUM: $f_1 + f_2 = f_0$
 $f_1 = 50 \text{ kHz}; f_2 = 39.91 \text{ kHz}$

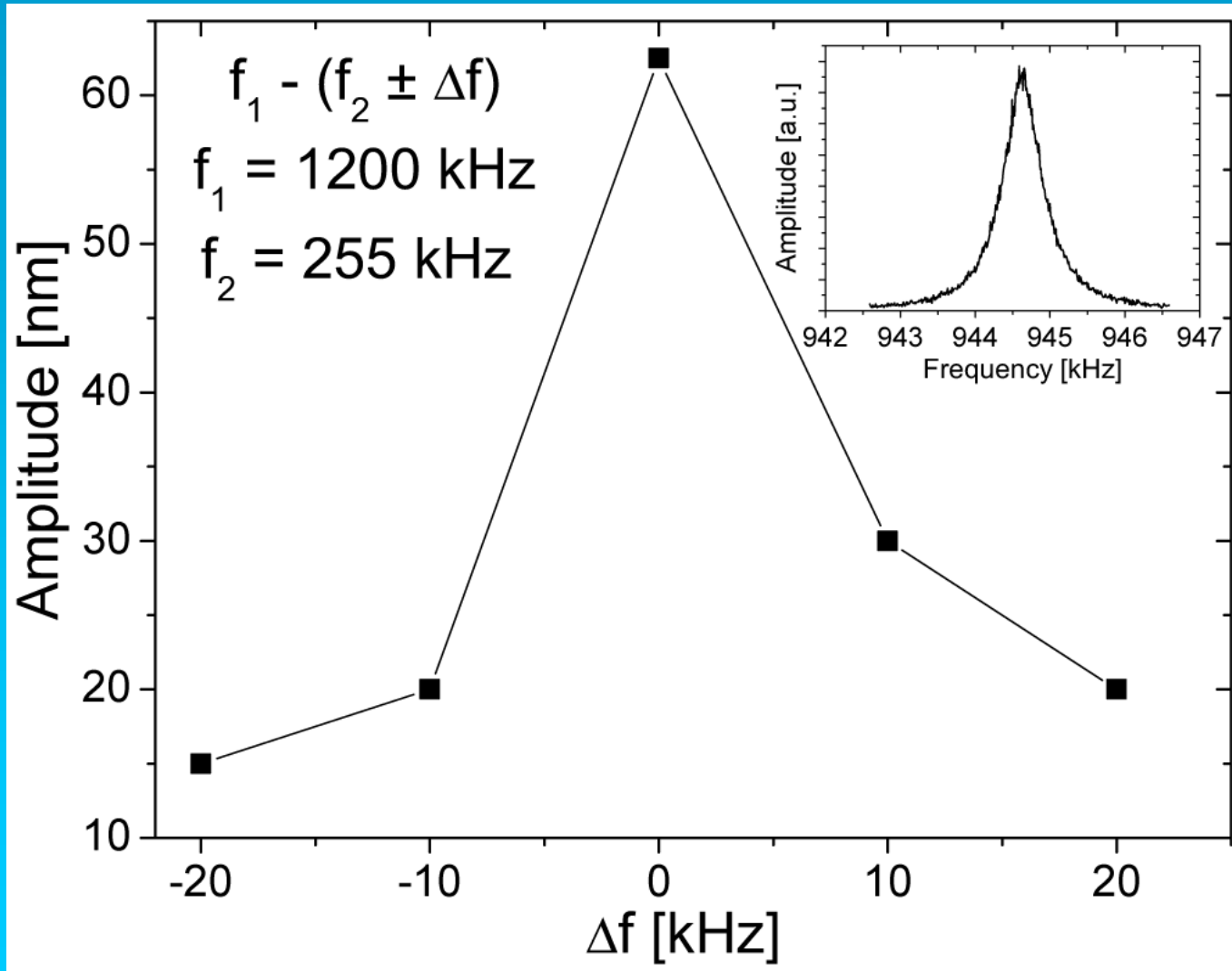


DIFFERENCE: $f_1 - f_2 = f_0$
 $f_1 = 1200 \text{ kHz}; f_2 = 255 \text{ kHz}$

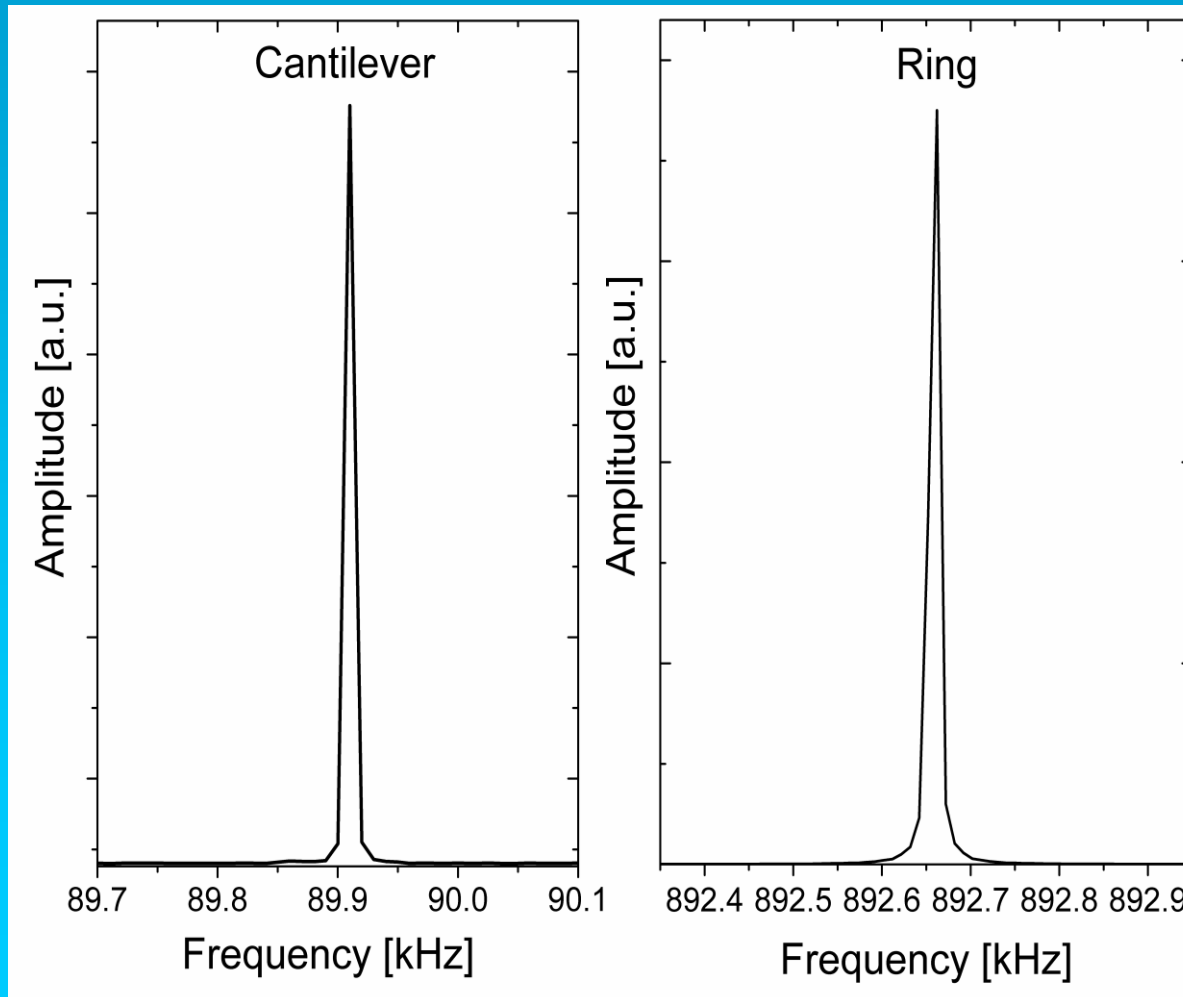


Elec. Letts., 46, 62-63, (2010)

Effect of changing f_2



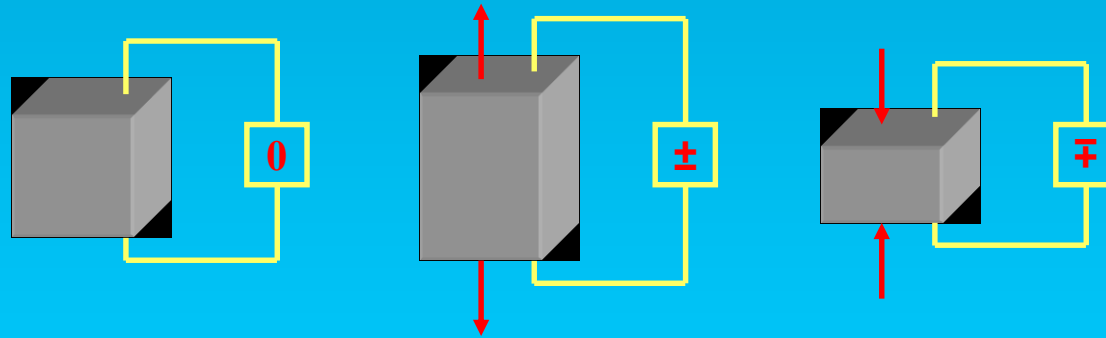
Electro-thermal mixing measurements on Al/SiC structures - Mixing resonant peaks for a cantilever ($L = 200 \mu\text{m}$) and a ring ($D = 190 \mu\text{m}$)



Electrical sensing: piezoelectric

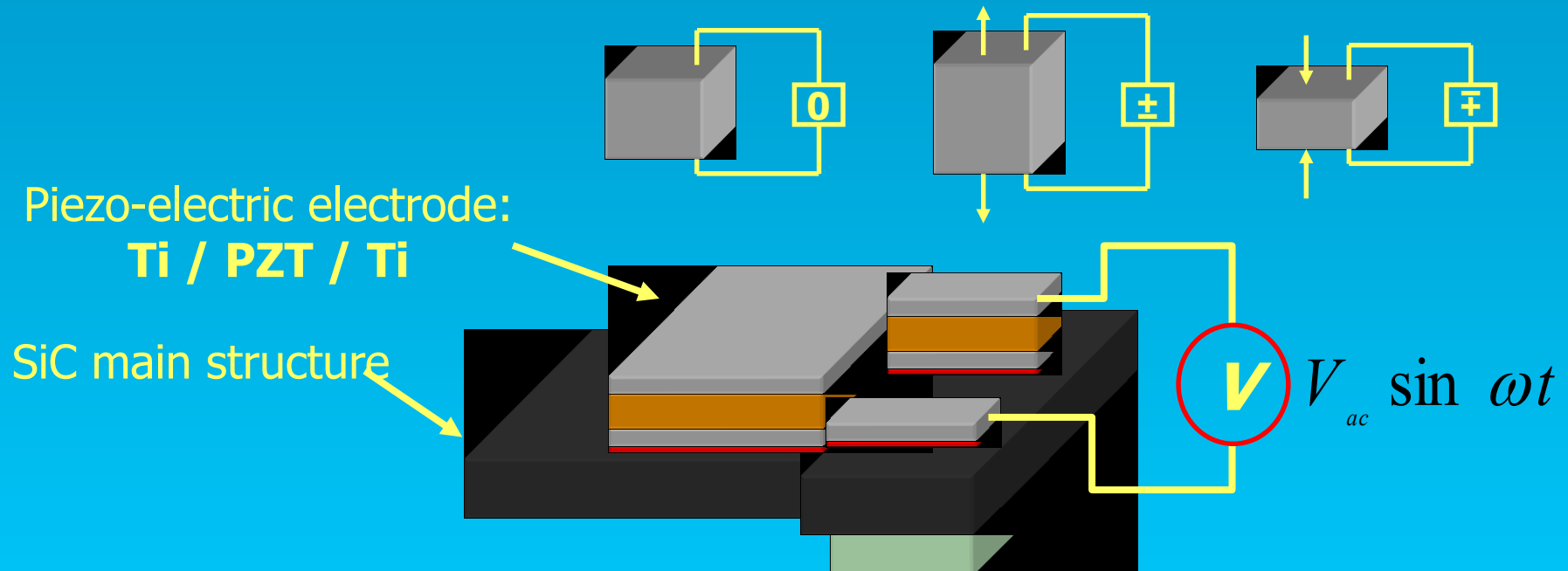
Piezoelectric effect:

Mechanical stress generates electrical potential



Piezo-electric actuation: theory

Mechanical stress \longleftrightarrow Electrical potential

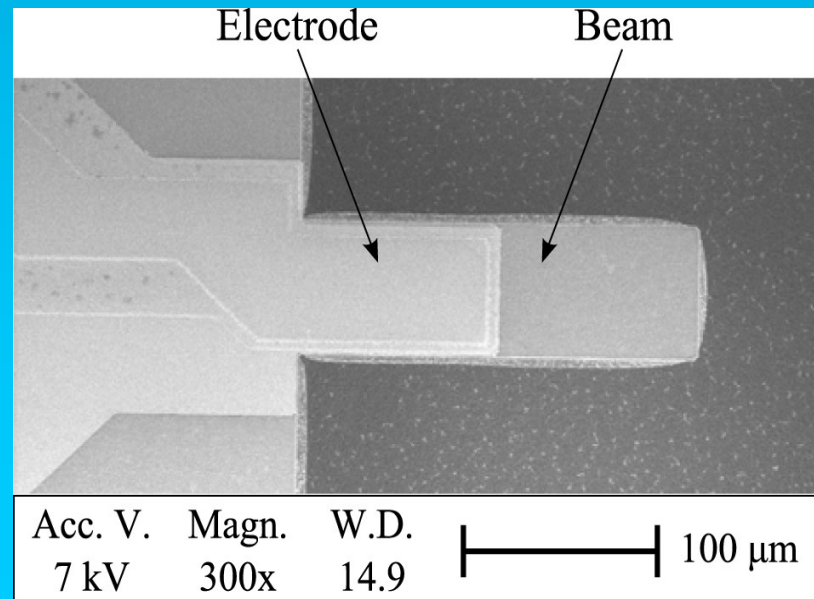
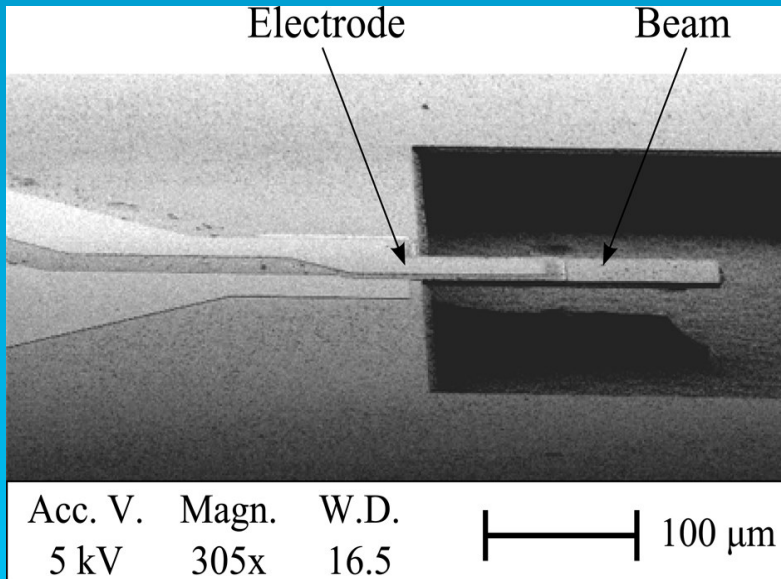


$$\text{Force} \propto \text{Electric field} \propto \text{Voltage}$$

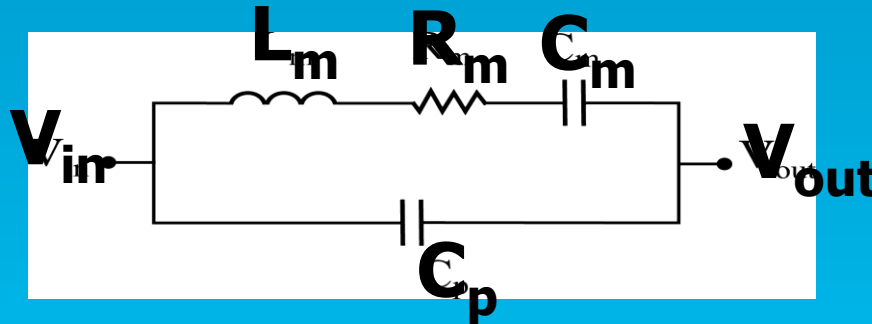
Resonance

$$f = \frac{\omega}{2\pi} = f_0$$

Piezoelectric resonators

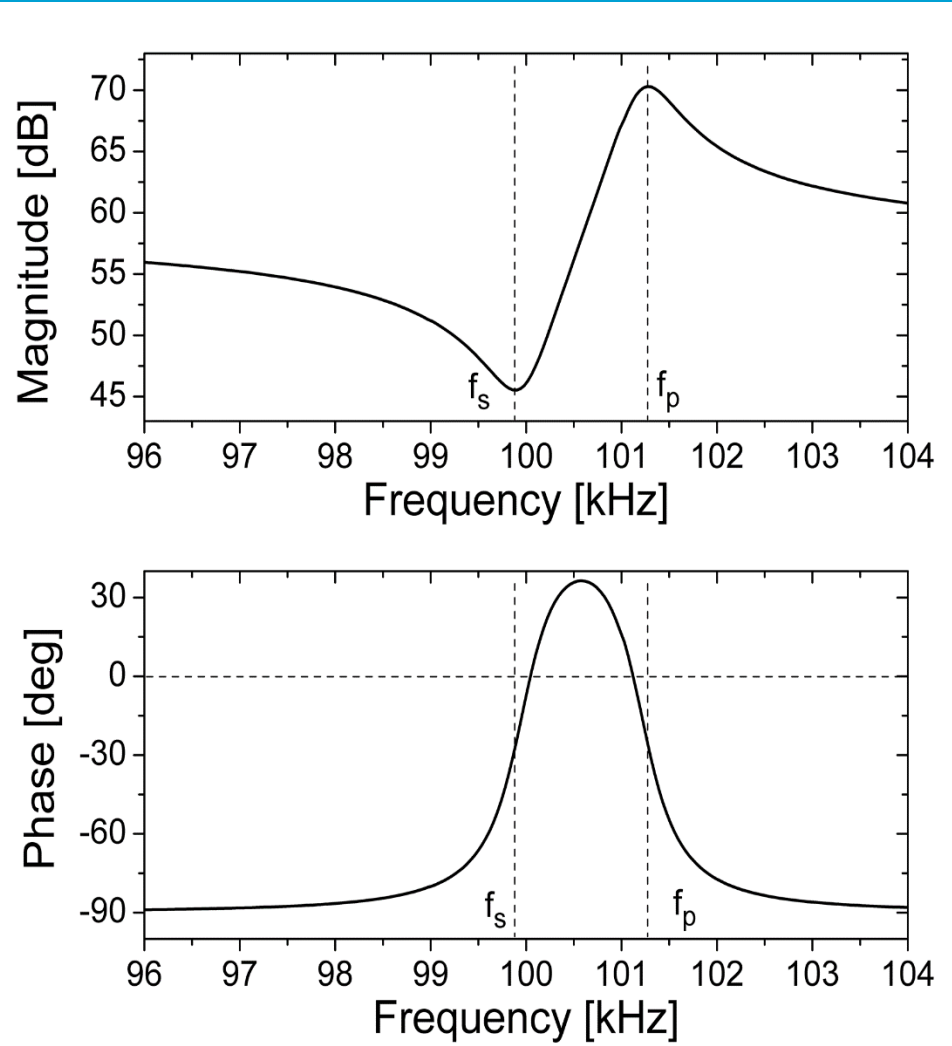


Butterworth-Van Dyke equivalent representation for electro-mechanical resonators



The electrical output of the equivalent circuit has been investigated by studying the impedance as a function of the frequency for different values of C_p (feedthrough capacitance)

Butterworth-Van Dyke equivalent representation for electro-mechanical resonators

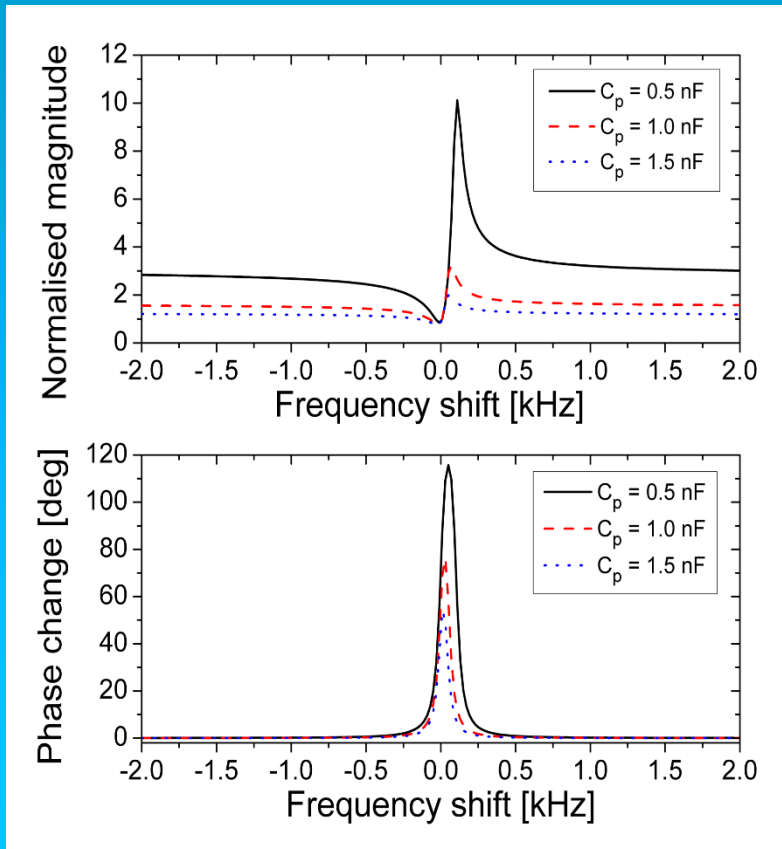


$$f_s \approx \frac{1}{2\pi \sqrt{L_m C_m}}$$

$$f_p \approx \frac{1}{2\pi \sqrt{L_m \frac{C_m C_p}{C_m + C_p}}}$$

Equivalent circuit analysis

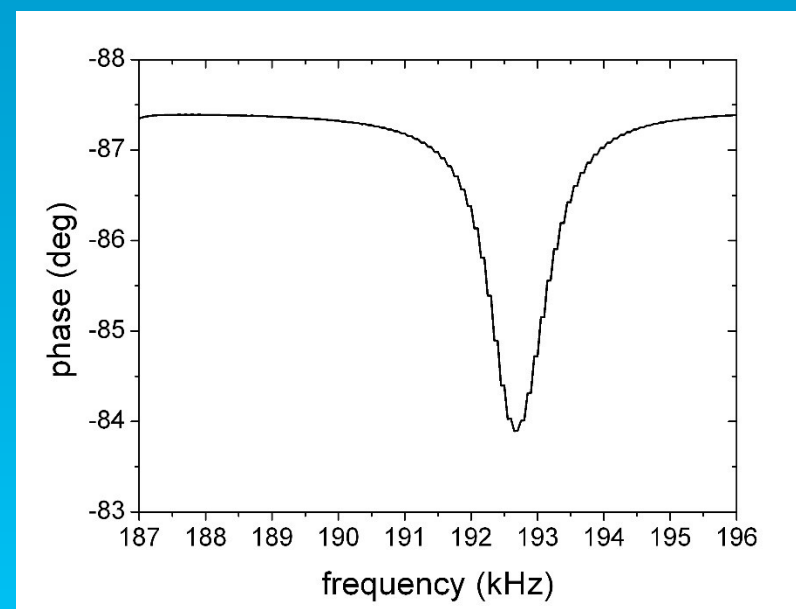
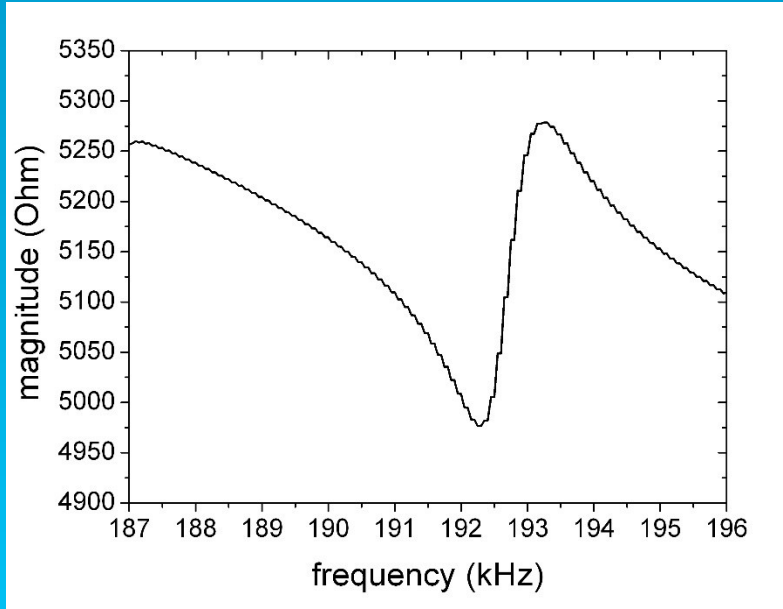
Simulations



Series resonance → C_m

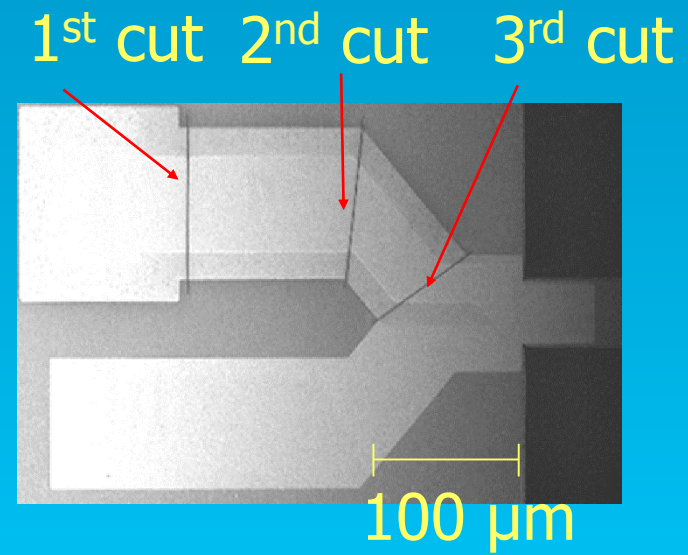
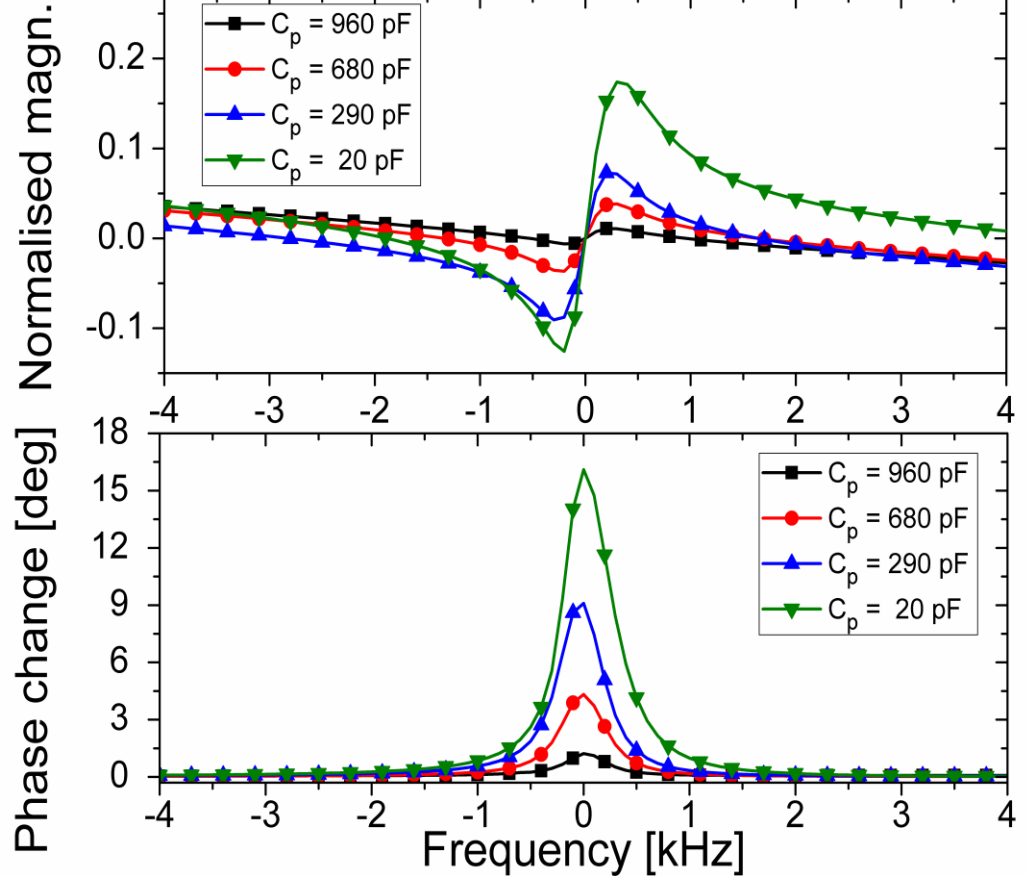
Parallel resonance → C_m and C_p

Piezoelectric resonators



Magnitude and phase of a silicon carbide resonator at 192.7 kHz detected with PZT stack; to be published in *J. Vac. Sci. Technol.*, 2010

Effect of C_p – Experimental



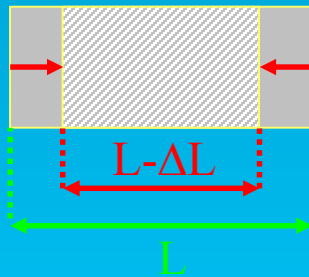
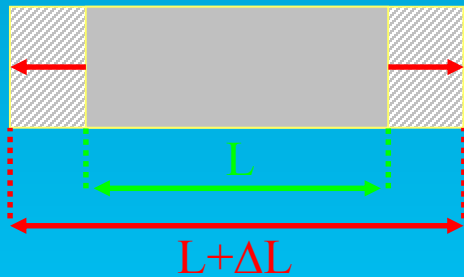
Electrode cuts performed by Focused Ion Beam to decrease C_p

$C_p \downarrow \rightarrow$ Electrical output \uparrow

Electrical sensing: piezoresistive

Piezoresistive effect:

Mechanical stress causes resistance change



$$\frac{\Delta R}{R} = K_S \frac{\Delta L}{L}$$

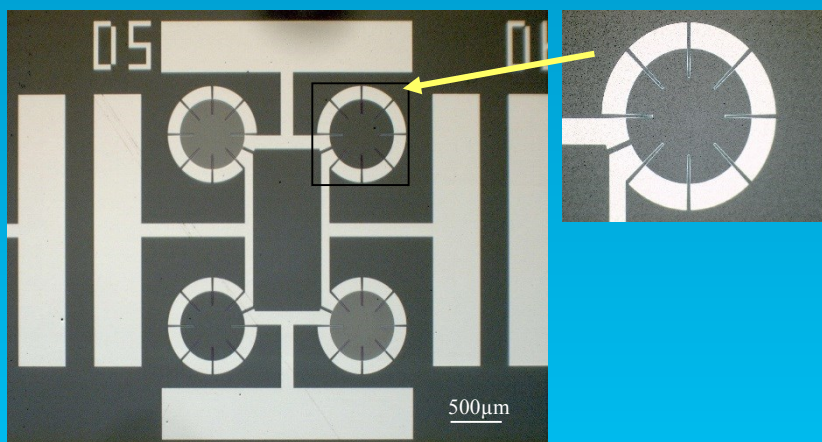
Gauge factor

Need of high gauge factor because of low vibration amplitudes

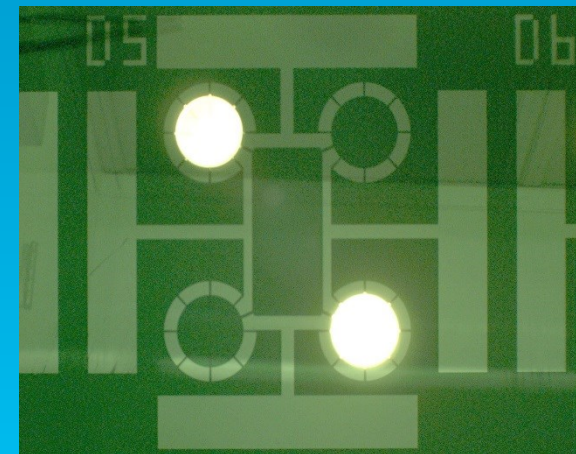
1. Doped poly-Si ($K_S = 200$)
2. Carbon nanotubes ($K_S = 600 - 1000$)

Pressure sensors

Pressure sensors

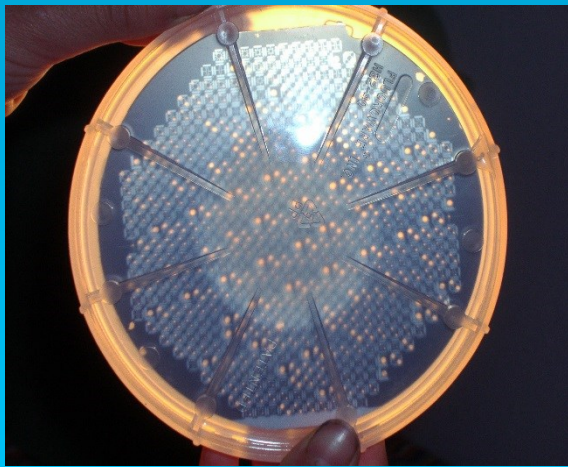


Pressure sensors 500 microns in diameter with Wheatstone bridge configuration under normal illumination

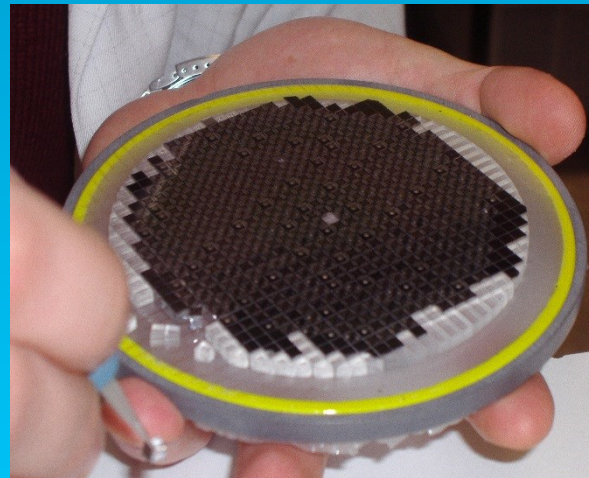


Pressure sensors 500 microns in diameter with Wheatstone bridge configuration under backlight illumination

Pressure sensors

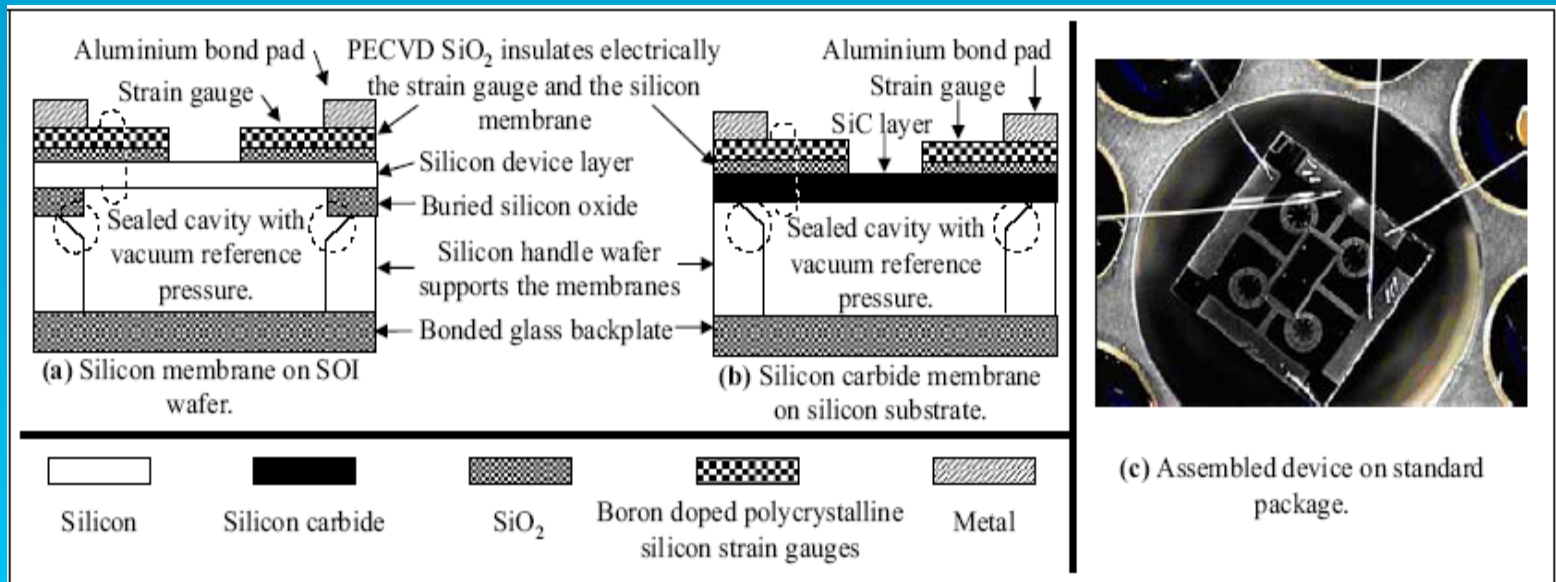


Whole wafer with
membrane sizes from
100 - 1200 microns



Bonded (Si to
glass) and diced
wafer

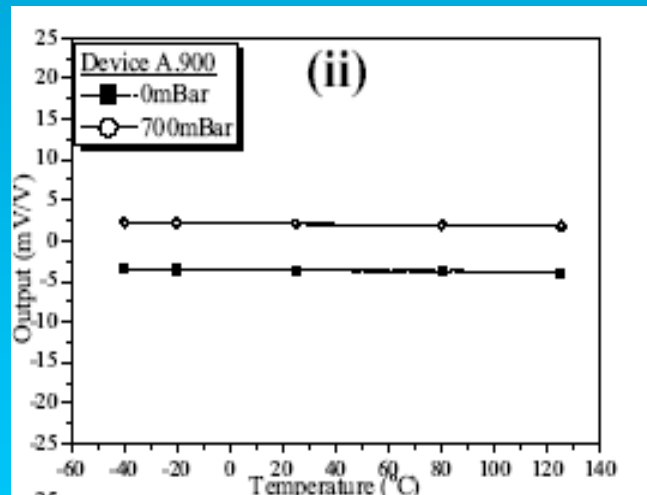
Pressure sensors



Sealed pressure sensor device a) SOI, b) SiC/Si,
c) packaged device

Pressure sensors

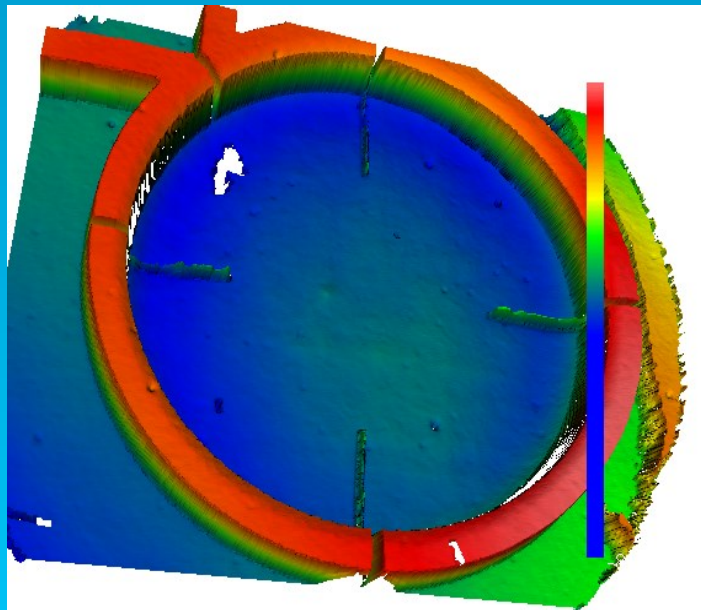
Good hysteresis performance between -40 and 130 degrees C



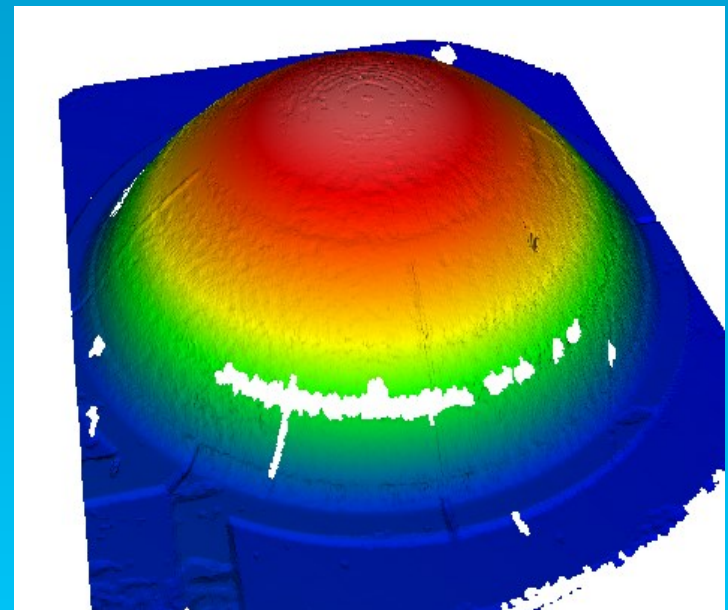
Type	Device identification	Device sensitivity (mV/V/mBar)
Silicon	C.900	3.63×10^{-3}
	C.400/A.400	2.84×10^{-3}
	A.900	2.98×10^{-3}
3C-SiC	C.900	3.25×10^{-3}

Sensitivity of Si and SiC membrane pressure sensors at room temperature between 0mBar and 700mBar

Pressure sensors

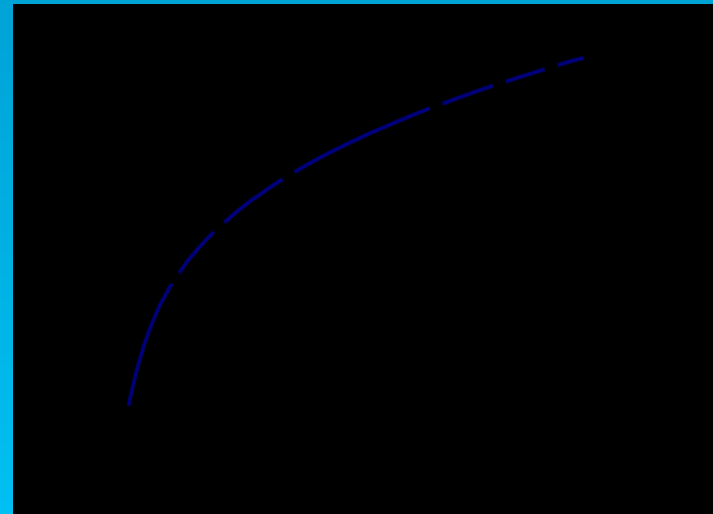
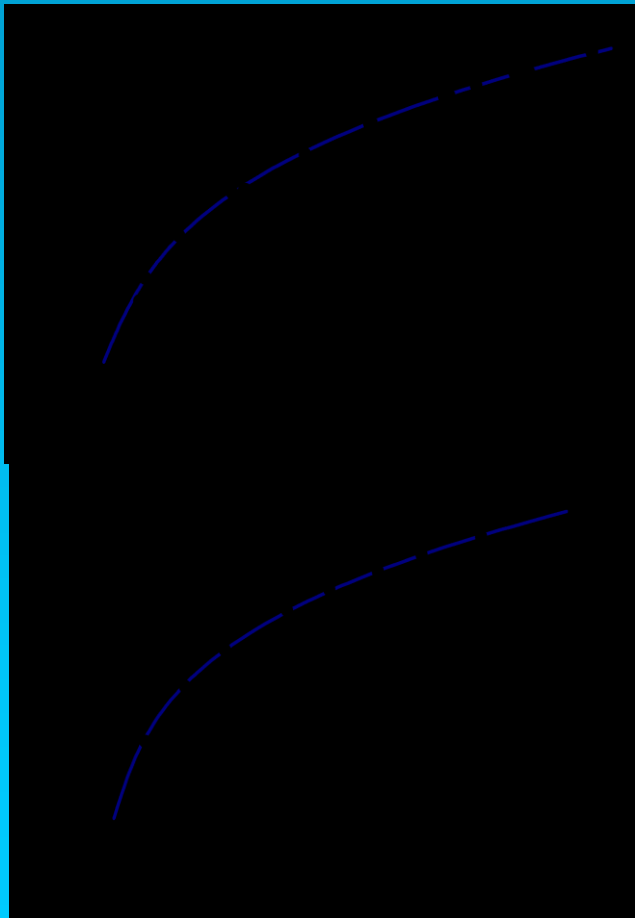


No Pressure Differential
Room Temperature – 500
micron membrane



1500mBar
differential
Temperature = 800
K

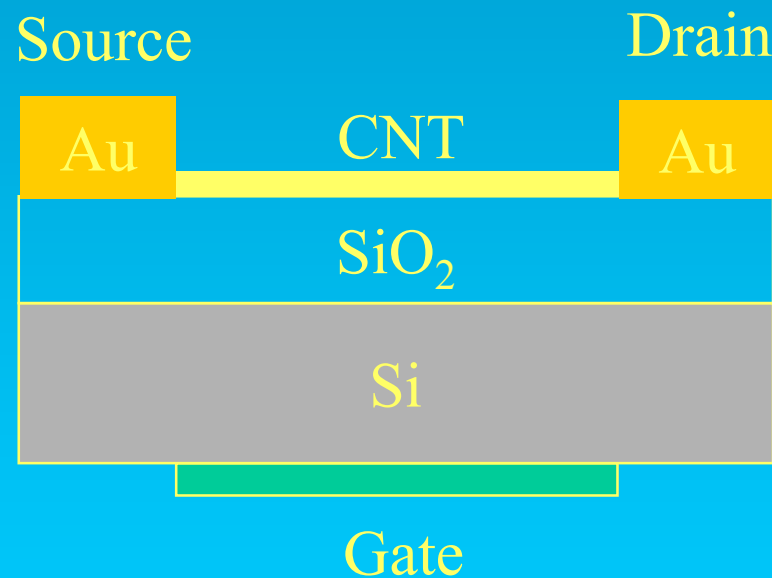
Deflection versus Pressure



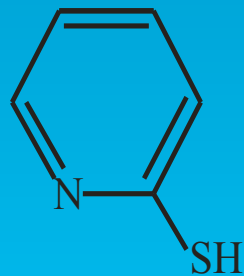
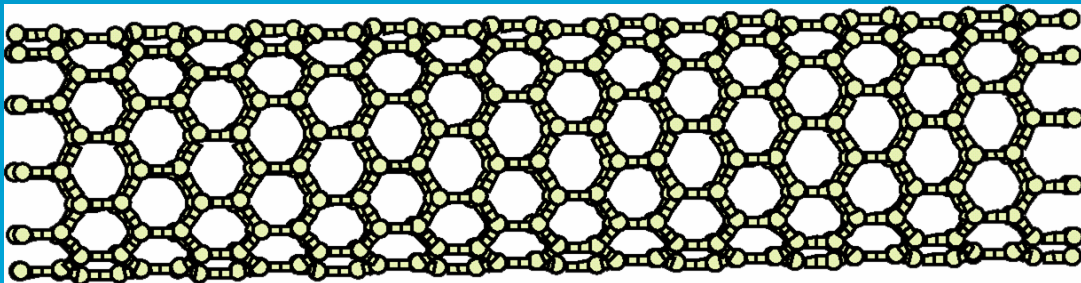
Height of Apex (deflection)
vs. Pressure Differential
Open symbols are the return
path (i.e. P decreasing)

Nanotube self-assembly

High yield carbon nanotube self-assembly for devices



*J. Vac. Sci. and Technol. B23, pp
3178 - 3181, (2005)*



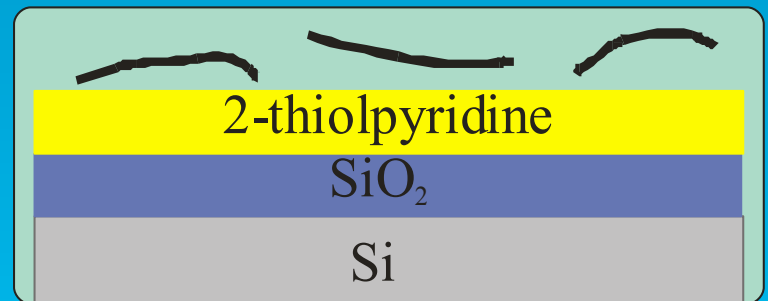
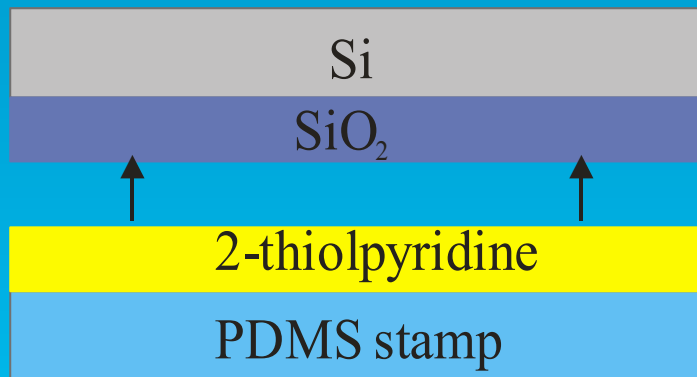
$\pi-\pi$

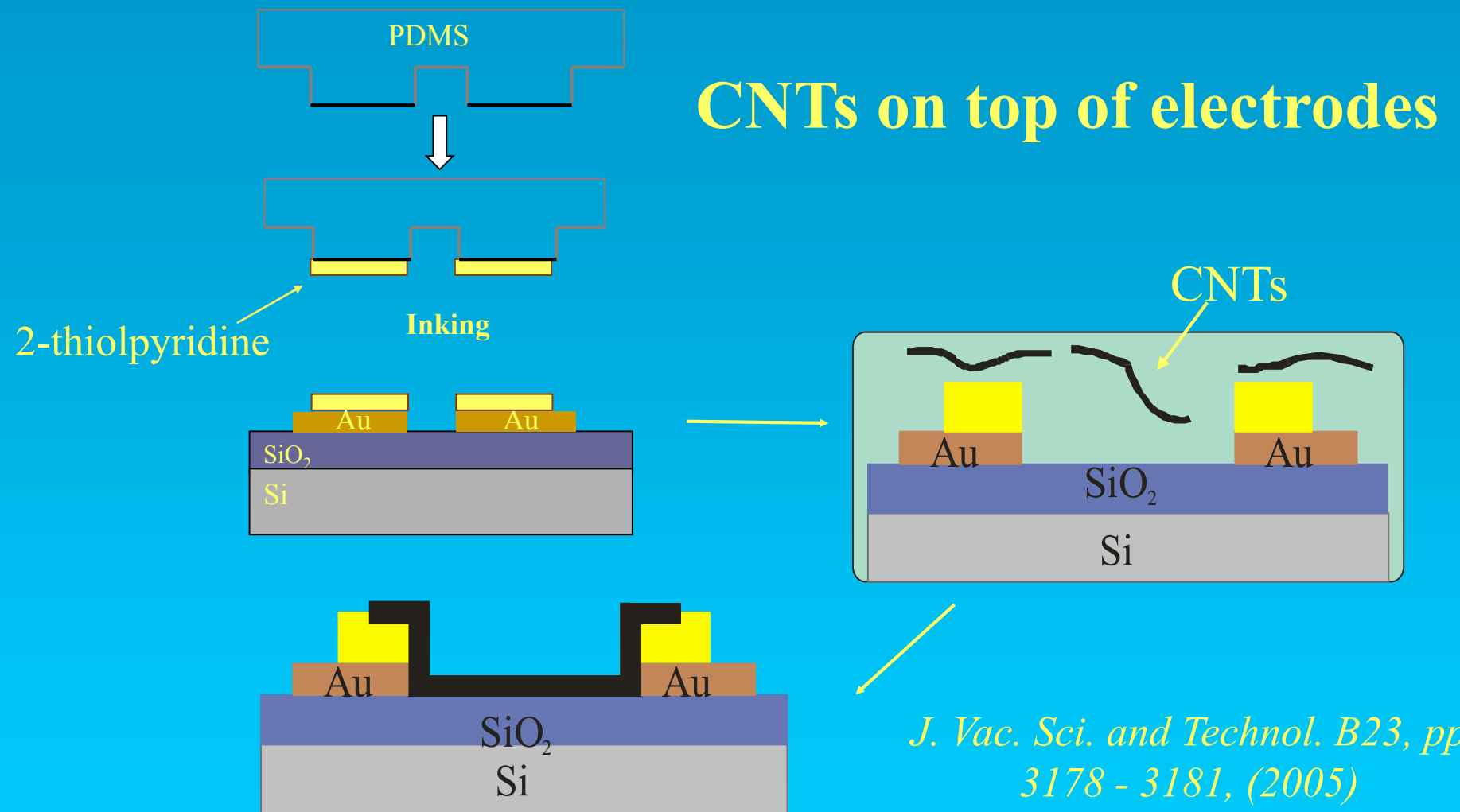
2-thiolpyridine

SiO_2

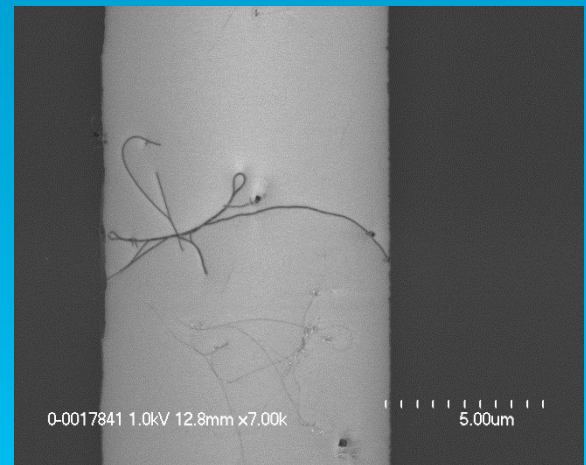
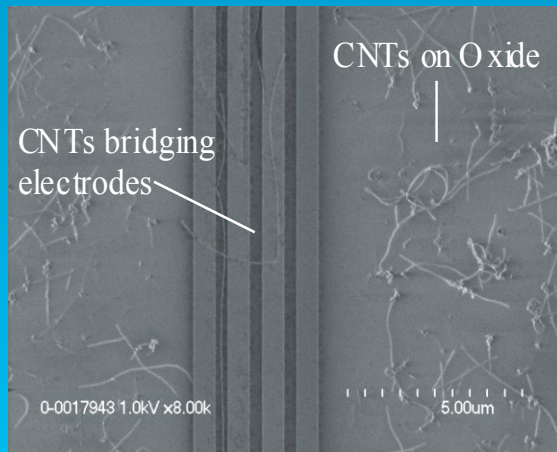
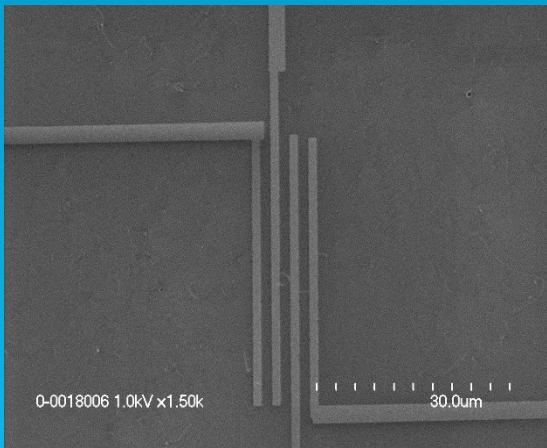
Si

Self-assembly: Electrodes on top of CNTs





Self-assembly

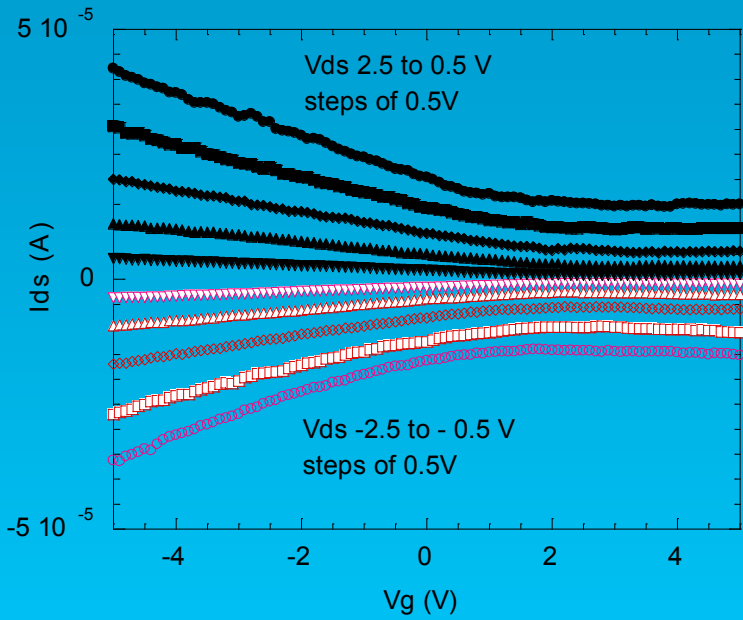


Electrodes

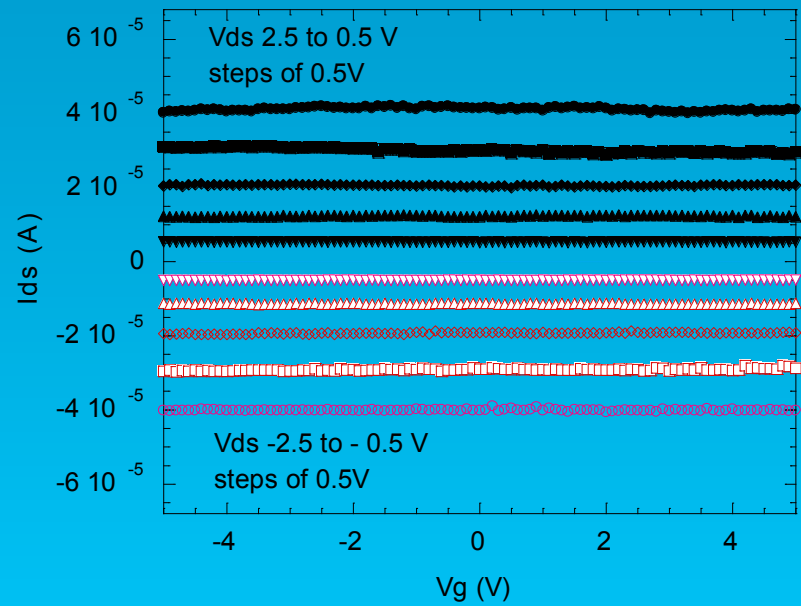
Electrodes on top of tubes

Tubes on top of electrodes

Gated I-V characteristics

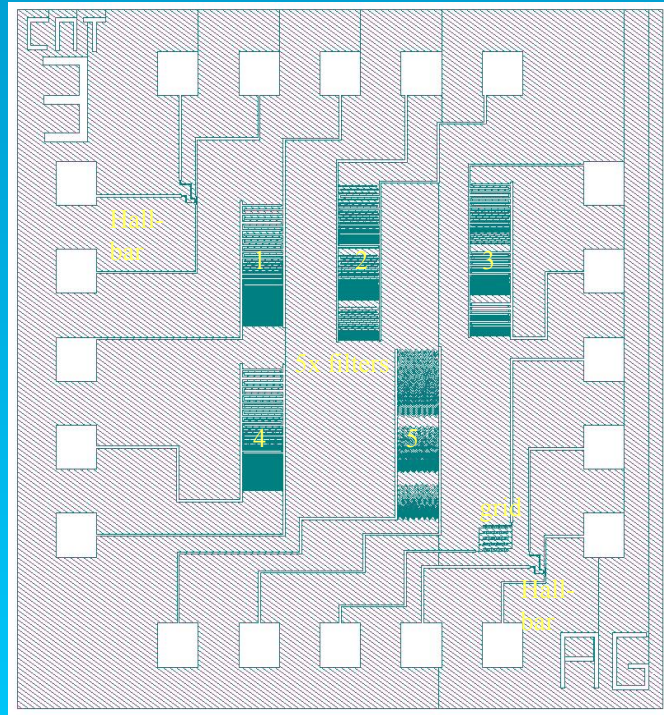


500nm gap electrodes on top of CNTs: p-type semiconducting

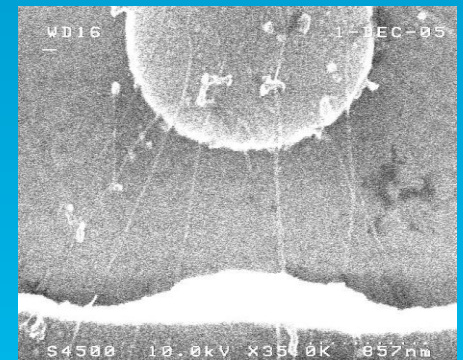
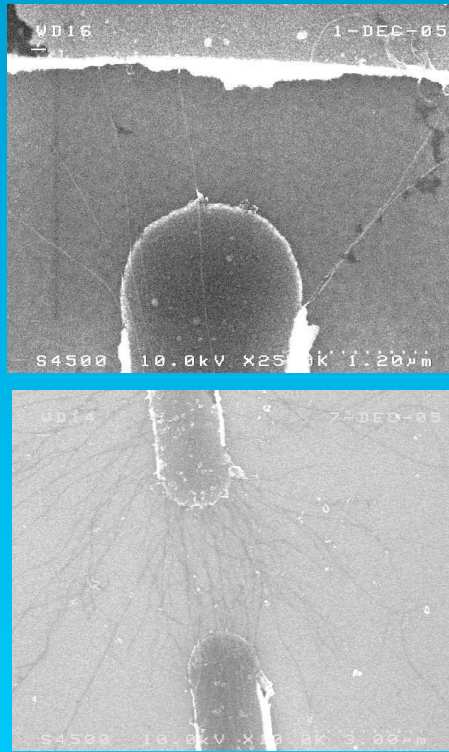


CNTs on top of 500nm gap electrodes: metallic

Dielectrophoresis



Electrode design



10 MHz 10 V

100 kHz 10 V

Emerging Fabrication Techniques

- Colloidal lithography

SiC nano-pillars fabrication

Colloidal lithography

Polystyrene micro-spheres dispersed in DI water

Lift-off lithography



1) Micro-sphere deposition



2) Titanium evaporation



3) Removal of micro-sphere (lift-off)



4) Oxide etching

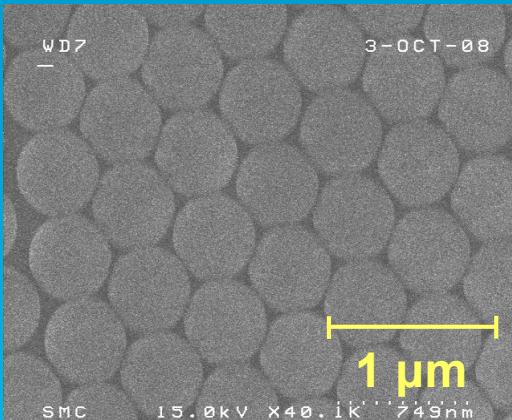


5) Removal of Ti and SiC etching

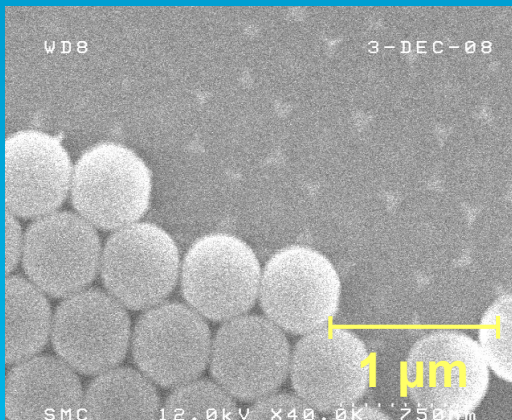


6) Removal of oxide

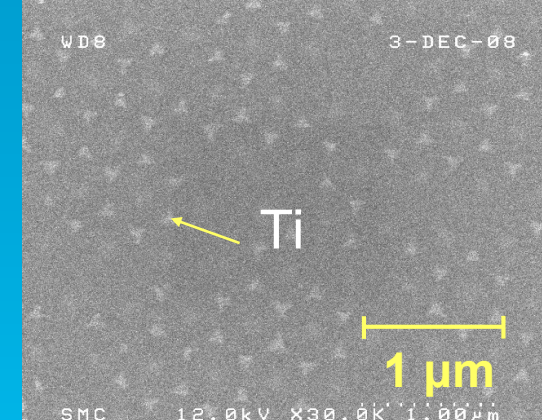
SiC nano-pillars fabrication



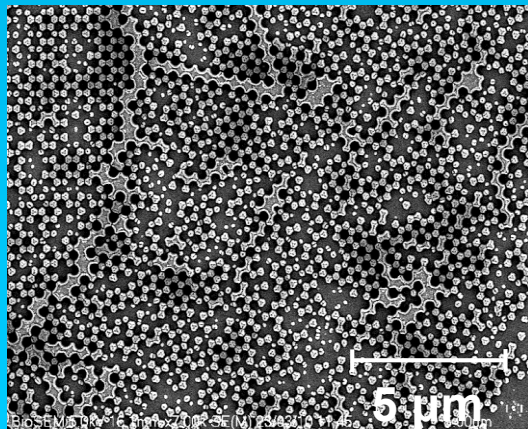
Deposited micro-spheres



Removal of micro-spheres

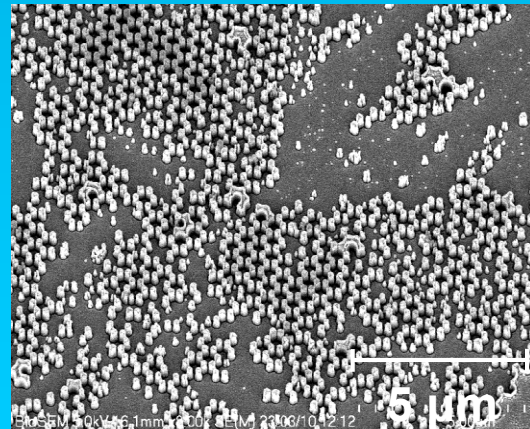


Micro-spheres removed



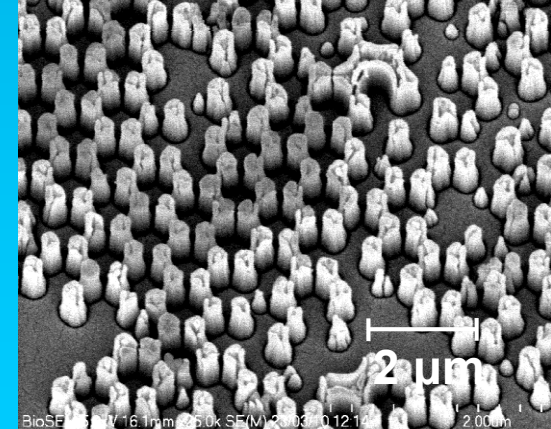
After SiC etching (tilt 0°)

MDP 4



After SiC etching (tilt 25°)

R.Cheung



After SiC etching (tilt 25°)

55